Supplement of Atmos. Chem. Phys., 23, 10191–10205, 2023
https://doi.org/10.5194/acp-23-10191-2023-supplement

Atmospheric Chemistry and Physics
Open Access
EGU

Supplement of

The atmospheric fate of 1,2-dibromo-4-(1,2-dibromoethyl)cyclohexane (TBECH): spatial patterns, seasonal variability, and deposition to Canadian coastal regions

Jenny Oh et al.

Correspondence to: Frank Wania (frank.wania@utoronto.ca)

Table of Contents

Text S1 Details on passive air sampling

86 and 83 passive air samplers (PASs) were obtained from Quebec (QC) and British Columbia (BC), respectively (Table S1). In QC, there were three deployment periods across 71 unique sites (Figure S1 right panel), with 48 PASs deployed from November 2019 to August 2020, 13 replicate PASs from August 2020 to July 2021, and 23 PASs and two replicate PASs from July 2021 to May 2022. In BC, there were three deployment periods across 47 unique sites (Figure S1 left panel), with 25 PASs and one replicate PAS deployed from October 2020 to November 2020, 23 PASs from August 2021 to February 2022, and 35 replicate PASs from July 2020 to April 2022. In Table S1, PASs deployed at the same site a second and third time are designated by _2, _3, etc.

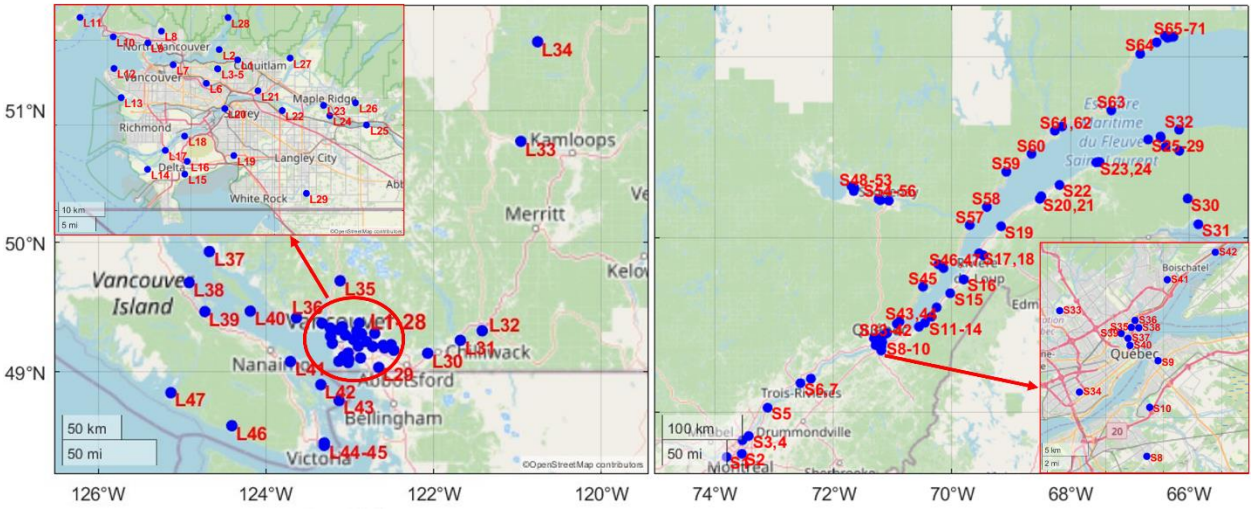

Figure S1 Maps with the passive air sampling sites and their codes in British Columbia (left) and Quebec (right). The inset map in the upper left shows the Vancouver metropolitan region.

Some sites were situated in the most urban and industrialized coastal cities of Canada, including the Vancouver metropolitan area (L3–7, L12, and L13; population ca. 2 400 000), Victoria, BC (L44 and 45); population ca. 360 000) on the west coast, and the Island of Montreal (S1–4; population ca. 3 600 000) and Quebec City, QC (S8–10 and S33–42; population ca. 700 000) on the east coast. Other sites were located in less densely populated areas, such as Saguenay, QC (S54–46; population ca. 100 000), or in remote regions, such as the shores of the outer St. Lawrence Estuary (S63). Population statistics were obtained from Statistics Canada (2021).

Table S1 Information on the passive air samples taken in Quebec and British Columbia: Geographical coordinates, deployment and retrieval date, deployment period, average temperature during the deployment period, population within a 20-km radius (NASA, 2015), and measured air concentrations of TBECH and BDE-47 in pg/m^3. Average temperature recordings are tabulated for sites used in temperature dependence and diffusive air-water gas exchange analyses.

Site name	Latitude	Longitude	Deployment date	Retrieval date	Deployment period (d)	Temperature (°C)	Population	α-TBECH	β-TBECH	BDE-47
Quebec										
S1	45.469155	-73.800449	2021-10-14	2022-05-21	219		2156606	0.39	0.30	2.52
S2	45.505762	-73.543673	2019-11-25	2020-08-17	266		2595043	1.21	0.73	2.17
S2_2	45.505762	-73.543673	2020-08-17	2021-07-27	344			0.83	0.61	1.64
S3	45.665733	-73.533969	2019-11-25	2020-08-17	266		1919061	0.61	0.52	1.50
S4	45.71537	-73.428631	2019-11-25	2020-08-16	265		779009	0.23	<LOD	1.64
S5	46.047893	-73.109854	2019-11-25	2020-08-16	265		73646	0.48	<LOD	1.42
S6	46.333255	-72.554767	2019-11-24	2020-08-16	266		166537	0.24	<LOD	1.28
S6_2	46.333255	-72.554767	2020-08-16	2021-07-27	345			0.19	0.26	0.70
S7	46.386946	-72.378962	2020-09-22	2021-07-27	308		147941	<LOD	<LOD	<LOD
S8	46.711971	-71.190931	2019-11-24	2020-08-15	265		631572	<LOD	<LOD	2.15
S8_2	46.711971	-71.190931	2020-08-15	2021-07-28	347			<LOD	<LOD	1.53
S9	46.805711	-71.174908	2019-11-24	2020-08-15	265		733757	0.26	0.20	2.26
S10	46.760038	-71.18688	2019-11-24	2020-08-15	265		712517	0.19	<LOD	1.02
S10_2	46.760038	-71.18688	2020-08-15	2021-07-28	347			0.12	0.18	1.02
S11	46.986643	-70.556641	2019-11-26	2020-08-14	262		19957	<LOD	<LOD	1.21
S12	47.032257	-70.455028	2019-11-26	2020-08-14	262		20322	<LOD	<LOD	0.63
S13	47.10166	-70.34451	2019-11-26	2020-08-14	262		14689	<LOD	<LOD	1.35
S14	47.207559	-70.257261	2019-11-26	2020-08-14	262		11461	<LOD	<LOD	0.63
S15	47.369697	-70.028755	2019-11-26	2020-08-13	261		14359	<LOD	<LOD	1.65
S16	47.527509	-69.802918	2019-11-26	2020-08-13	261		12300	<LOD	<LOD	1.06
S17	47.823721	-69.541425	2019-11-26	2020-08-13	261		32407	0.11	<LOD	1.17
S18	47.800518	-69.468863	2019-11-26	2020-08-13	261		32877	<LOD	<LOD	0.83
S18_2	47.800518	-69.468863	2020-08-13	2021-07-26	347			<LOD	<LOD	0.86
S19	48.128717	-69.169932	2019-11-27	2020-08-13	260		9121	<LOD	<LOD	0.70
S19_2	48.128717	-69.169932	2020-08-13	2021-07-26	347			<LOD	<LOD	0.75
S20	48.436658	-68.516966	2019-11-27	2020-08-10	257		55712	<LOD	<LOD	1.30
S21	48.464097	-68.492452	2019-11-27	2020-08-10	257		55238	0.11	<LOD	0.85
S22	48.591288	-68.184971	2019-11-27	2020-08-11	258		17606	0.18	0.14	0.82
S23	48.84196	-67.564692	2019-11-27	2020-08-11	258		17956	0.20	<LOD	<LOD
S24	48.845968	-67.507684	2019-11-27	2020-08-11	258		18321	<LOD	<LOD	0.96
S25	49.095121	-66.690157	2019-11-27	2020-08-11	258		8135	<LOD	0.14	1.00
S25_2	49.095121	-66.690157	2020-08-11	2021-08-01	355			<LOD	<LOD	0.81
S26	49.12794	-66.480661	2019-11-28	2020-08-12	258		9330	<LOD	<LOD	1.00
S26_2	49.12794	-66.480661	2021-08-02	2022-05-06	277			0.67	0.53	<LOD
S27	49.118923	-66.47789	2021-08-02	2022-05-06	277		9333	<LOD	<LOD	<LOD
S28	49.013853	-66.394871	2021-08-02	2022-05-06	277		7333	<LOD	<LOD	<LOD
S29	48.970136	-66.162999	2021-08-02	2022-05-06	277		344	<LOD	<LOD	<LOD
S30	48.439206	-66.02294	2021-08-02	2022-05-06	277		180	<LOD	<LOD	<LOD
S31	48.150858	-65.8442	2021-08-02	2022-05-06	277		11847	<LOD	<LOD	<LOD
S32	49.203244	-66.167248	2019-11-28	2020-08-12	258		2154	<LOD	<LOD	<LOD
S32_2	49.203244	-66.167248	2020-08-12	2021-08-01	354			<LOD	<LOD	<LOD
S33	46.854722	-71.315556	2019-11-24	2020-08-18	268		743965	0.12	0.34	1.10
S34	46.774955	-71.287295	2019-11-25	2020-09-24	304		744469	0.44	0.37	1.06
S35	46.838333	-71.213333	2019-11-25	2020-08-19	268		734119	0.29	<LOD	1.67
S35_2	46.838333	-71.213333	2020-08-19	2021-07-28	343			0.13	<LOD	0.72
S36	46.845162	-71.207898	2021-07-28	2022-05-02	278		733503	0.37	0.18	0.66
S37	46.82762	-71.217761	2021-07-28	2022-05-02	278		741534	0.82	0.99	1.04
S38	46.837912	-71.202403	2021-07-28	2022-05-02	278		732965	0.54	0.47	0.72
S39	46.832376	-71.227689	2021-07-28	2022-05-02	278		739729	0.53	0.47	0.78

S40	46.820679	-71.215028	2021-07-28	2022-05-02	278		747332	0.63	0.48	0.80
S41	46.885	-71.161667	2019-11-25	2020-08-19	268		663439	<LOD	0.15	2.00
S42	46.91182	-71.093094	2019-11-25	2020-08-20	269		479747	0.20	<LOD	1.03
S43	47.020833	-70.927778	2019-11-25	2020-08-20	269		33302	0.11	0.17	1.07
S43_2	47.02268	-70.927039	2021-07-28	2022-05-02	278			0.22	0.75	1.10
S44	47.045278	-70.883056	2019-11-25	2020-08-20	269		25802	<LOD	<LOD	1.44
S45	47.445193	-70.488035	2019-11-26	2020-08-21	269		12877	<LOD	<LOD	0.94
S46	47.655946	-70.143002	2019-11-26	2020-08-21	269		14453	0.15	<LOD	1.14
S47	47.697467	-70.226313	2019-11-26	2020-08-21	269		15173	<LOD	<LOD	1.07
S48	48.551334	-71.644332	2019-11-27	2020-08-22	269		48382	<LOD	<LOD	6.10
S48_2	48.551334	-71.644332	2020-08-22	2021-07-30	342			<LOD	<LOD	0.60
S49	48.523285	-71.655464	2019-11-27	2020-08-22	269		50440	<LOD	<LOD	1.12
S50	48.575821	-71.69414	2021-07-30	2022-05-03	277		45685	0.18	0.18	<LOD
S51	48.558106	-71.654878	2021-07-30	2022-05-03	277		47839	0.41	0.43	<LOD
S52	48.566261	-71.653343	2021-07-30	2022-05-03	277		46623	0.52	0.68	<LOD
S53	48.561596	-71.64784	2021-07-30	2022-05-03	277		47875	0.16	0.32	<LOD
S54	48.433506	-71.237773	2019-11-27	2020-08-22	269		136328	<LOD	<LOD	1.68
S54_2	48.433506	-71.237773	2020-08-22	2021-07-29	341			<LOD	<LOD	<LOD
S55	48.419938	-71.208286	2019-11-27	2020-08-23	270		137601	<LOD	<LOD	0.76
S56	48.41706	-71.064918	2019-11-27	2020-08-23	270		149037	0.19	<LOD	0.96
S57	48.141483	-69.699112	2019-11-29	2020-08-24	269		3198	<LOD	<LOD	0.98
S58	48.344593	-69.410547	2019-11-29	2020-08-24	269		2829	<LOD	0.22	1.03
S59	48.73751	-69.0827	2019-11-29	2020-08-24	269		4377	<LOD	<LOD	<LOD
S60	48.936019	-68.656616	2019-11-30	2021-07-30	608		3306	<LOD	<LOD	<LOD
S61	49.191401	-68.264497	2019-11-30	2020-08-25	269		27138	<LOD	<LOD	1.16
S62	49.237981	-68.142384	2019-11-30	2020-08-25	269		23863	<LOD	0.16	<LOD
S62_2	49.237981	-68.142384	2020-08-25	2021-07-31	340			<LOD	<LOD	<LOD
S63	49.415035	-67.311237	2019-12-01	2020-08-25	268		458	<LOD	<LOD	0.59
S64	50.031046	-66.823474	2019-12-01	2020-08-25	268		7002	<LOD	<LOD	0.72
S65	50.154989	-66.54716	2021-07-31	2022-05-04	277		26023	0.23	0.33	<LOD
S66	50.220751	-66.363786	2019-12-01	2020-08-26	269		28021	<LOD	<LOD	0.96
S66_2	50.220751	-66.363786	2020-08-26	2021-07-31	339			<LOD	<LOD	<LOD
S67	50.2249	-66.406352	2021-07-31	2022-05-04	277		28023	0.43	0.50	<LOD
S68	50.204196	-66.363854	2021-07-31	2022-05-04	277		28061	0.65	0.58	<LOD
S69	50.212716	-66.312511	2021-07-31	2022-05-04	277		27614	0.16	<LOD	<LOD
S70	50.216136	-66.262451	2021-07-31	2022-05-04	277		27602	0.50	0.37	<LOD
S71	50.206686	-66.353095	2021-07-31	2022-05-04	277		27892	<LOD	<LOD	<LOD
British Columbia										
L1	49.29467	-122.860722	2020-03-04	2020-08-18	167	13.3	1635872	1.58	1.21	5.18
L1_2	49.2946	-122.860722	2020-08-18	2021-03-26	220	8.3		1.12	0.92	1.58
L1_3	49.2946	-122.860722	2021-03-26	2021-08-16	143	15.2		1.98	2.12	5.02
L2	49.314809	-122.916119	2021-05-17	2021-12-03	200	14.6	1603159	0.82	0.53	1.26
L3	49.27724	-122.92025	2020-01-23	2020-06-17	146	6.5	1875070	0.65	0.63	2.38
L3_2	49.27724	-122.92025	2020-06-17	2020-11-20	156	13.9		0.98	0.70	4.90
L3_3	49.27724	-122.92025	2020-11-20	2021-04-29	160	6.0		0.44	0.39	2.72
L3_4	49.27724	-122.92025	2021-10-01	2022-04-04	185	5.7		0.34	0.25	2.32
L4	49.277425	-122.92093	2020-06-17	2020-11-20	156	13.9	1892985	0.78	0.57	2.60
L4_2	49.277425	-122.92093	2020-11-20	2021-04-29	160	6.0		0.58	0.43	2.13
L4_3	49.2774	-122.92093	2021-04-29	2021-10-01	155	16.7		0.61	0.66	2.13
L4_4	49.277425	-122.92093	2021-10-01	2022-04-04	185	5.7		0.41	0.23	1.78
L5	49.27742	-122.92093	2020-06-17	2020-11-20	156	13.9	1892985	0.70	0.55	2.26
L5_2	49.27742	-122.92093	2020-11-20	2021-04-29	160	6.0		0.43	0.43	2.24
L5_3	49.2771	-122.92099	2021-04-29	2021-10-01	155	16.7		0.58	0.70	1.44
L5_4	49.27742	-122.92093	2021-10-01	2022-04-04	185	5.7		0.49	0.65	2.13
L6	49.249106	-122.954593	2021-05-12	2021-12-04	206	14.4	2012036	0.78	0.65	2.31
L7	49.28514	-123.05381	2021-05-03	2021-10-03	153	16.7	1695810	2.20	1.59	5.46
L7_2	49.28514	-123.05381	2021-10-03	2022-04-06	185	5.7		0.61	0.54	0.92
L8	49.35072	-123.089058	2020-02-16	2020-10-16	243	12.3	1196091	0.63	0.34	1.74
L9	49.327892	-123.12952	2021-05-25	2021-12-03	192	14.7	1260721	0.77	0.55	2.57
L10	49.3398	-123.2333	2020-10-05	2021-05-14	221	7.0	911872	0.57	0.54	3.67

L10_2	49.3398	-123.2333	2021-05-14	2021-12-03	203	14.6		1.23	1.15	1.45
L11	49.377486	-123.332887	2021-05-15	2021-12-05	204	14.6	357701	1.05	0.78	1.33
L12	49.278051	-123.231074	2021-05-26	2021-12-04	192	14.7	1184810	0.71	0.63	1.01
L13	49.22104	-123.20958	2020-06-23	2020-11-16	146	14.7	1286814	1.14	0.88	3.38
L13_2	49.22104	-123.20958	2020-11-16	2021-05-04	169	6.0		0.56	0.68	0.97
L13_3	49.22104	-123.20958	2021-05-04	2021-12-04	214	14.4		0.76	0.80	1.65
L14	49.080669	-123.130664	2021-06-03	2021-12-05	185	14.7	929072	1.29	1.11	3.53
L15	49.07119	-123.019187	2020-05-08	2020-09-29	144	16.2	1226050	0.59	0.46	1.96
L16	49.096479	-123.0120251	2021-08-24	2022-02-24	184	7.0	1573731	0.44	<LOD	2.11
L17	49.11788	-123.07748	2021-05-04	2021-12-04	214	14.4	1562783	0.34	0.24	2.50
L18	49.14582	-123.0198175	2021-08-24	2022-02-24	184	7.0	1865239	0.68	0.65	0.90
L19	49.107833	-122.872199	2021-06-30	2022-01-21	205	10.8	1509064	0.58	0.47	1.00
L20	49.199489	-122.8991932	2021-08-24	2022-02-24	184	7.0	2068510	0.44	0.28	1.25
L21	49.234653	-122.800053	2021-05-12	2021-12-16	218	13.6	1509339	0.95	0.73	3.02
L22	49.1958	-122.72716	2021-05-06	2021-12-16	224	13.6	1264596	0.63	0.57	2.07
L23	49.20579	-122.60346	2021-05-06	2021-12-16	224	13.6	778091	0.62	0.55	1.65
L24	49.18588	-122.58501	2021-05-06	2021-12-16	224	13.6	744309	0.23	0.27	1.08
L25	49.167454	-122.474923	2021-06-03	2021-12-16	196	14.7	439299	0.57	0.32	2.16
L26	49.210922	-122.507831	2021-05-12	2021-12-03	205	14.4	436915	0.33	0.17	1.21
L27	49.298214	-122.703625	2021-06-04	2021-12-03	182	14.7	802039	0.80	0.52	1.65
L28	49.377252	-122.889298	2021-05-17	2021-12-03	200	14.6	987976	0.87	0.63	1.62
L29	49.03365	-122.65477	2021-05-04	2021-12-04	214	14.4	648376	0.31	0.20	1.40
L30	49.143885	-122.070985	2021-08-27	2022-02-28	185	7.0	202088	0.18	<LOD	1.02
L31	49.24474	-121.681236	2020-02-27	2020-10-10	226	13.7	32557	<LOD	<LOD	1.02
L31_2	49.24474	-121.681236	2020-10-10	2021-06-18	251	8.0		0.17	<LOD	<LOD
L31_3	49.24474	-121.681236	2021-06-18	2022-03-13	268	10.3		<LOD	<LOD	<LOD
L32	49.31884	-121.420888	2020-02-15	2020-10-10	238	12.3	7565	<LOD	<LOD	1.26
L32_2	49.31884	-121.420888	2021-05-23	2022-04-30	342	10.3		<LOD	<LOD	<LOD
L33	50.76738	-120.958617	2020-02-27	2020-10-09	225	13.7	1428	0.21	0.19	1.02
L34	51.51144	-120.759003	2020-05-23	2020-10-13	143	15.6	1438	<LOD	<LOD	0.62
L34_2	51.51144	-120.759003	2020-10-13	2021-05-20	219	7.4		0.14	0.21	<LOD
L34_3	51.51144	-120.759003	2021-05-20	2021-10-10	143	17.0		0.34	0.34	10.24
L35	49.70542	-123.116055	2020-02-28	2020-09-22	207	13.7	19253	0.40	0.29	1.05
L36	49.41939	-123.637475	2020-02-18	2020-10-17	242	12.3	26645	0.32	0.18	1.12
L36_2	49.41939	-123.637475	2020-10-07	2021-05-21	226	7.4		<LOD	0.21	0.65
L37	49.92998	-124.67645	2020-02-21	2020-08-04	165	12.3	15575	0.27	<LOD	0.64
L38	49.6914	-124.9178	2020-06-07	2020-11-15	161	14.8	60955	0.27	0.28	1.10
L39	49.4673	-124.7299	2020-05-24	2020-10-25	154	15.6	9653	0.48	0.15	1.64
L39_2	49.4673	-124.7299	2020-10-25	2021-06-02	220	7.4		0.16	0.26	0.83
L39_3	49.4673	-124.7299	2021-06-02	2022-01-21	233	11.7		0.20	0.26	1.36
L40	49.47106	-124.188079	2020-06-20	2021-01-29	223	11.3	17248	0.25	0.32	1.64
L40_2	49.47106	-124.188079	2021-01-29	2021-10-01	245	12.9		0.26	0.26	<LOD
L41	49.0787	-123.70913	2020-04-14	2021-02-18	310	11.4	53069	0.39	0.38	1.46
L41_2	49.0787	-123.70913	2021-02-18	2021-09-07	201	12.5		0.45	0.87	<LOD
L42	48.8983	-123.34592	2020-07-12	2021-04-18	280	9.9	15431	0.29	0.41	0.84
L42_2	48.8983	-123.34592	2021-04-18	2021-12-01	227	14.1		0.35	0.34	0.75
L43	48.7753	-123.12827	2020-05-28	2020-10-11	136	16.9	8251	0.16	<LOD	1.77
L43_a_1	48.7753	-123.12827	2020-07-02	2021-04-03	275	9.9		0.19	<LOD	<LOD
L43_a_2	48.7753	-123.12827	2021-04-03	2021-11-26	237	13.8		0.23	0.17	0.60
L43_b_1	48.7753	-123.12827	2020-07-02	2021-04-03	275	9.9		0.18	<LOD	0.73
L43_b_2	48.7753	-123.12827	2021-04-03	2021-11-26	237	13.8		0.26	0.51	0.79
L43_c_1	48.7753	-123.12827	2020-07-02	2021-04-03	275	9.9		0.14	0.17	0.81
L43_c_2	48.7753	-123.12827	2021-04-03	2021-11-26	237	13.8		0.15	0.13	0.84
L44	48.421	-123.3049	2020-05-06	2020-10-04	151	16.2	314981	0.73	0.57	2.30
L44_2	48.421	-123.3049	2020-10-04	2021-05-29	237	7.4		0.27	0.28	1.59
L44_3	48.421	-123.30	2021-05-29	2021-10-08	132	17.8		0.50	0.30	1.20
L45	48.4406	-123.3054	2020-04-13	2020-10-03	173	15.1	317955	1.49	1.13	6.49
L45_2	48.4406	-123.3054	2020-10-03	2021-05-29	238	7.4		0.51	0.50	1.48
L45_3	48.4406	-123.3054	2021-05-29	2021-10-10	134	17.8		0.89	0.72	1.98
L46	48.57619	-124.407916	2020-10-23	2021-08-04	285	9.5	255	0.25	<LOD	0.76
L47	48.83573	-125.135358	2020-10-27	2021-06-23	239	8.3	251	0.24	0.20	3.03

Table S2 Information on the active air sampling (AAS) on Saturna Island, BC, Tadoussac, QC, and Toronto, ON: The start date of each collection period, the air concentrations in pg/m^3 of TBECH and BDE-47 in the gas phase, the average sea surface temperature (SST in °C), the average air temperature (AAT in °C), and the CO air concentration in µg/m^3 predicted by FLEXPART.

Start Date	α-TBECH	β-TBECH	BDE-47	SST[a]	AAT[b]	Predicted CO
Saturna Island, BC						
2019-12-18	<LOD	<LOD	0.61	6.1	10.5	4.16
2020-01-17	0.06	<LOD	0.39	2.2	9.0	2.12
2020-02-14	0.06	0.04	0.23	4.9	8.6	1.26
2020-03-15	0.13	0.07	<LOD	3.8	8.3	3.01
2020-05-11	0.06	0.04	0.87	15.4	10.8	3.50
2020-06-11	<LOD	<LOD	1.08	13.7	12.4	2.18
2020-07-08	<LOD	<LOD	0.92	14.0	13.9	0.66
2020-08-06	0.13	0.12	0.57	18.3	16.5	0.81
2020-09-05	0.11	0.05	0.58	14.6	16.5	2.21
2020-10-03	0.11	<LOD	0.41	13.3	15.8	6.00
2020-11-01	0.10	0.06	0.30	9.2	13.6	7.11
Tadoussac, QC						
2020-12-18	0.09	0.05	0.13	0.2	-10.0	2.3
2021-01-16	0.04	0.02	<LOD	-0.3	-2.0	5.63
2021-02-14	<LOD	<LOD	<LOD	-0.7	-11.8	1.48
2021-03-13	0.02	<LOD	<LOD	0.0	-11.8	1.18
2021-04-14	0.05	0.02	0.06	4.0	4.3	1.57
2021-05-15	0.10	<LOD	0.10	7.0	6.8	2.00
2021-06-13	0.23	0.15	0.20	10.4	11.0	1.37
2021-07-12	0.29	0.17	0.61	12.5	15.8	1.01
2021-08-10	0.22	0.13	0.39	12.8	18.0	5.40
2021-09-08	0.08	0.06	0.69	12.7	14.0	4.68
2021-10-07	<LOD	<LOD	0.33	10.4	11.0	1.94
2021-11-05	0.14	0.07	<LOD	7.6	3.8	2.12
Toronto, ON						
2020-06-17	0.80	0.56	5.26		25.2	7.20
2020-06-24	0.75	0.55	6.20		25.2	4.37
2020-07-01	0.69	0.46	3.96		29.2	4.60
2020-07-08	0.68	0.37	9.26		27.0	5.04
2020-07-15	0.63	0.49	4.09		26.3	4.98
2020-07-22	1.34	0.87	4.05		27.0	4.43
2020-07-29	0.30	0.19	1.40		24.9	5.06
2020-08-05	0.80	0.48	4.49		25.4	5.26
2020-08-12	0.36	0.26	1.27		24.5	5.08

2020-08-19	0.78	0.56	3.16	26.5	5.56
2020-08-26	0.45	0.25	1.56	23.4	4.96
2020-09-02	0.54	0.34	2.31	20.8	4.76
2020-09-09	0.33	0.17	1.03	19.1	5.62
2020-09-16	0.43	0.26	2.02	17.4	6.27
2020-09-23	0.54	0.36	1.45	21.1	7.39
2020-09-30	0.35	0.22	0.97	15.0	4.81
2020-10-07	0.30	0.20	0.93	14.7	4.52
2020-10-14	0.23	0.20	0.90	12.6	5.56
2020-10-21	0.19	0.14	0.50	10.8	6.41
2020-10-28	0.22	0.14	0.41	7.2	5.04
2020-11-04	0.61	0.57	1.06	14.7	7.42
2020-11-11	0.22	0.12	0.40	7.2	5.28
2020-11-18	0.22	0.13	0.29	6.8	5.91
2020-11-25	0.27	0.19	0.75	6.6	6.88
2020-12-02	0.23	0.14	0.33	2.5	4.52
2020-12-09	0.25	0.20	0.43	3.3	6.18
2020-12-16	0.30	0.21	0.51	1.9	6.62
2020-12-23	0.29	0.22	0.46	2.2	4.08
2020-12-30	0.31	0.21	0.27	2.8	10.36
2021-01-06	0.29	0.18	0.31	1.5	6.25
2021-01-13	0.33	0.22	0.47	3.1	6.60
2021-01-20	0.25	0.17	0.27	0.4	4.65
2021-01-27	0.18	0.11	0.48	-2.7	3.62
2021-02-03	0.26	0.14	0.37	-1.9	5.00
2021-02-10	0.20	0.11	0.16	-3.9	4.45
2021-02-17	0.36	0.24	0.41	0.1	6.56
2021-02-24	0.21	0.14	0.35	2.5	5.26
2021-03-03	0.29	0.18	0.57	2.4	4.88
2021-03-10	0.21	0.11	0.42	5.1	4.63
2021-03-17	0.44	0.25	0.71	8.0	6.20
2021-03-24	0.27	0.14	0.63	9.5	5.21
2021-03-31	0.28	0.15	0.61	9.3	6.06
2021-04-07	0.19	0.15	0.69	12.9	7.72
2021-04-14	0.32	0.22	0.58	10.9	3.39
2021-04-21	0.27	0.19	0.31	12.9	5.72
2021-04-28	0.25	0.16	0.96	11.6	6.10
2021-05-05	0.25	0.15	0.41	12.6	2.43
2021-05-12	0.80	0.51	1.65	19.7	6.14

[a] SST values were taken from the NOAA CoastWatch/OceanWatch database (ACSPO Global SST from AHI).

[b] AAT values were provided by Saturna CAPMON, Pointe de l'Islet, and University of Toronto Scarborough for sites on Saturna Island, Tadoussac, and Toronto, respectively.

Table S3 Information of precipitation sampling: Precipitation concentrations and wet deposition fluxes of TBECH and BDE-47in pg/L and pg/m^2/day, respectively, collected in Saturna Island, BC and in Tadoussac, QC.

Start Date	End Date	Concentration (pg/L)			Wet deposition flux (pg/m^2/day)		
Saturna Island, BC		**α-TBECH**	**β-TBECH**	**BDE-47**	**α-TBECH**	**β-TBECH**	**BDE-47**
2019-12-18	2020-01-17	51	45	102	181	159	361
2020-01-17	2020-02-14	115	97	69	779	657	468
2020-02-14	2020-03-15	681	561	19	2099	1731	58
2020-03-15	2020-04-15	708	588	36	1048	870	53
2020-04-15	2020-05-11	236	191	14	351	285	21
2020-05-11	2020-06-11	55	48	10	84	72	15
2020-06-11	2020-07-08	231	176	12	277	211	14
2020-07-08	2020-08-06	1416	1125	<LOD	1035	823	<LOD
2020-08-06	2020-09-04	1150	943	23	991	813	20
2020-09-05	2020-10-03	718	589	21	1439	1181	42
2020-10-03	2020-11-01	67	54	50	207	167	156
2020-11-01	2020-12-01	141	113	44	615	491	192
Tadoussac, QC							
2020-12-18	2021-01-16	67	51	90	114	87	153
2021-01-16	2021-02-14	12	12	58	19	19	92
2021-02-14	2021-03-13	22	19	64	28	25	82
2021-03-13	2021-04-14	189	151	25	283	226	38
2021-04-14	2021-05-15	289	224	26	628	487	56
2021-05-15	2021-06-13	302	251	45	197	163	29
2021-06-13	2021-07-12	34	29	22	96	82	63
2021-07-12	2021-08-10	116	95	43	177	144	66
2021-08-10	2021-09-08	72	49	32	44	30	19
2021-09-08	2021-10-07	24	20	30	78	64	96
2021-10-07	2021-11-05	11	11	27	36	35	89

Table S4 Detection frequencies (DFs), LODs, and LOQs of the target brominated/halogenated flame retardants in the passive air samplers and passive water samplers. The LODs and LOQs of each compound are in ng/sample.

Compound	PAS			PWS		
	DF (%)	LOD	LOQ	DF (%)	LOD	LOQ
BDE-17	5	0.005	0.02	79	0.005	0.02
BDE-28	3	0.01	0.04	77	0.01	0.03
BDE-49	0	0.06	0.19	0	1.29	4.32
BDE-66	1	0.04	0.13	23	0.03	0.09
BDE-71	0	0.04	0.12	0	0.88	2.94
BDE-85	8	0.09	0.29	0	0.09	0.29
BDE-99	4	0.07	0.23	85	0.04	0.14
BDE-100	0	0.19	0.62	77	0.01	0.02
BDE-138	0	0.07	0.25	0	0.06	0.20
BDE-153	0	0.07	0.24	15	0.04	0.12
BDE-154	1	0.01	0.04	27	0.01	0.04
BDE-183	0	0.03	0.10	4	0.02	0.05
BDE-190	26	0.09	0.29	8	0.04	0.14
BDE-209	1	0.19	0.63	13	0.18	0.59
ATE	5	0.06	0.20	0	0.05	0.16
BATE	0	0.03	0.09	0	0.03	0.09
PBBz	7	0.03	0.08	0	0.03	0.08
PBT	0	0.06	0.19	0	0.06	0.19
PBEB	0	0.05	0.17	0	0.05	0.17
DBTE	0	0.03	0.09	0	0.03	0.09
HBBz	7	0.11	0.35	0	0.11	0.35
EHTBB	0	0.11	0.36	0	0.11	0.36
BTBPE	0	0.14	0.47	0	0.14	0.47
BEHTBP	1	0.17	0.56	0	0.17	0.56
DBDPE	0	15.98	53.27	0	15.98	53.27
Dec-602	0	0.004	0.01	0	0.004	0.01
Dec-604	0	0.02	0.08	0	0.02	0.08
syn-DP	0	0.01	0.02	0	0.01	0.02
anti-DP	0	0.003	0.01	0	0.003	0.01

Table S5 Air concentrations, LODs, and LOQs of the polybrominated diphenyl ethers (PBDEs) in active air samples from Saturna Island, BC and Tadoussac, QC, in pg/m^3.

Start Date	PBDE congener concentration (pg/m^3)													
	17	**28**	**49**	**66**	**71**	**85**	**99**	**100**	**138**	**153**	**154**	**183**	**190**	**209**
Saturna Island, BC														
2019-12-18	<LOD	<LOD	<LOD	<LOD	<LOD	<LOD	<LOD	<LOD	<LOD	<LOD	<LOD	<LOD	<LOD	<LOD
2020-01-17	<LOD	<LOD	<LOD	<LOD	<LOD	<LOD	<LOD	<LOD	<LOD	<LOD	<LOD	<LOD	<LOD	<LOD
2020-02-14	<LOD	<LOD	<LOD	<LOD	<LOD	<LOD	<LOD	<LOD	<LOD	<LOD	<LOD	<LOD	<LOD	<LOD
2020-03-15	<LOD	<LOD	<LOD	<LOD	<LOD	<LOD	<LOD	<LOD	<LOD	<LOD	<LOD	<LOD	<LOD	<LOD
2020-05-11	<LOD	0.05	<LOD	<LOD	<LOD	<LOD	0.18	<LOD	<LOD	<LOD	<LOD	<LOD	<LOD	<LOD
2020-06-11	<LOD	0.10	<LOD	<LOD	<LOD	<LOD	0.51	<LOD	<LOD	<LOD	<LOD	<LOD	<LOD	<LOD
2020-07-08	<LOD	<LOD	<LOD	<LOD	<LOD	<LOD	0.50	<LOD	<LOD	<LOD	<LOD	<LOD	<LOD	<LOD
2020-08-06	<LOD	<LOD	<LOD	<LOD	<LOD	<LOD	0.58	<LOD	<LOD	<LOD	<LOD	<LOD	<LOD	<LOD
2020-09-05	<LOD	<LOD	<LOD	<LOD	<LOD	<LOD	<LOD	<LOD	<LOD	<LOD	<LOD	<LOD	<LOD	<LOD
2020-10-03	<LOD	<LOD	<LOD	<LOD	<LOD	<LOD	0.19	<LOD	<LOD	<LOD	<LOD	<LOD	<LOD	<LOD
2020-11-01	<LOD	<LOD	<LOD	<LOD	<LOD	<LOD	<LOD	<LOD	<LOD	<LOD	<LOD	<LOD	<LOD	<LOD
LOD	0.01	0.01	0.05	0.11	0.57	0.12	0.12	0.04	0.34	0.17	0.04	0.07	0.09	1.26
LOQ	0.02	0.02	0.17	0.36	1.89	0.42	0.42	0.13	1.13	0.57	0.14	0.22	0.31	4.21
Tadoussac, QC														
2020-12-18	<LOD	<LOD	<LOD	<LOD	<LOD	<LOD	<LOD	<LOD	<LOD	<LOD	<LOD	<LOD	<LOD	<LOD
2021-01-16	<LOD	<LOD	<LOD	<LOD	<LOD	<LOD	0.25	<LOD	<LOD	<LOD	<LOD	<LOD	<LOD	<LOD
2021-02-14	<LOD	<LOD	<LOD	<LOD	<LOD	<LOD	0.28	<LOD	<LOD	<LOD	<LOD	<LOD	<LOD	<LOD
2021-03-13	<LOD	<LOD	<LOD	<LOD	<LOD	<LOD	<LOD	<LOD	<LOD	<LOD	<LOD	<LOD	<LOD	<LOD
2021-04-14	<LOD	<LOD	<LOD	<LOD	<LOD	<LOD	<LOD	<LOD	<LOD	<LOD	<LOD	<LOD	<LOD	<LOD
2021-05-15	<LOD	<LOD	<LOD	<LOD	<LOD	<LOD	<LOD	<LOD	<LOD	<LOD	<LOD	<LOD	<LOD	<LOD
2021-06-13	<LOD	<LOD	<LOD	<LOD	<LOD	<LOD	<LOD	<LOD	<LOD	<LOD	<LOD	<LOD	<LOD	<LOD
2021-07-12	<LOD	<LOD	<LOD	<LOD	<LOD	<LOD	0.28	<LOD	<LOD	<LOD	<LOD	<LOD	<LOD	<LOD
2021-08-10	0.05	<LOD	<LOD	<LOD	<LOD	<LOD	<LOD	<LOD	<LOD	<LOD	<LOD	<LOD	<LOD	<LOD
2021-09-08	0.03	<LOD	<LOD	<LOD	<LOD	<LOD	0.22	<LOD	<LOD	<LOD	<LOD	<LOD	<LOD	<LOD
2021-10-07	<LOD	<LOD	<LOD	<LOD	<LOD	<LOD	0.25	<LOD	<LOD	<LOD	<LOD	<LOD	<LOD	<LOD
2021-11-05	<LOD	<LOD	<LOD	<LOD	<LOD	<LOD	0.40	<LOD	<LOD	<LOD	<LOD	<LOD	<LOD	<LOD
LOD	0.02	0.06	0.02	0.12	0.02	0.52	0.18	0.04	0.14	0.09	0.03	0.06	0.19	0.33
LOQ	0.06	0.21	0.07	0.41	0.07	1.74	0.60	0.14	0.46	0.30	0.10	0.19	0.63	1.10

Table S6 Air concentrations, LODs, and LOQs of the other brominated/halogenated flame retardants in active air samples from Saturna Island, BC and Tadoussac, QC, in pg/m^3.

Start Date	Concentration (pg/m^3)														
	ATE	**BATE**	**PBBz**	**PBT**	**PBEB**	**DBTE**	**HBBz**	**EHTBB**	**BTBPE**	**BEHTBP**	**DBDPE**	**Dec-602**	**Dec-604**	***syn*-DP**	***anti*-DP**
Saturna Island, BC															
2019-12-18	<LOD	<LOD	<LOD	<LOD	<LOD	0.19	<LOD	<LOD	<LOD	<LOD	<LOD	<LOD	<LOD	<LOD	<LOD
2020-01-17	<LOD	<LOD	<LOD	<LOD	<LOD	0.35	<LOD	<LOD	<LOD	<LOD	<LOD	<LOD	<LOD	<LOD	<LOD
2020-02-14	<LOD	<LOD	<LOD	<LOD	<LOD	0.45	<LOD	<LOD	<LOD	<LOD	<LOD	<LOD	<LOD	<LOD	<LOD
2020-03-15	<LOD	<LOD	<LOD	<LOD	<LOD	<LOD	<LOD	<LOD	<LOD	<LOD	<LOD	<LOD	<LOD	<LOD	<LOD
2020-05-11	<LOD	<LOD	<LOD	<LOD	<LOD	1.32	<LOD	<LOD	<LOD	<LOD	<LOD	<LOD	<LOD	<LOD	<LOD
2020-06-11	<LOD	<LOD	<LOD	<LOD	<LOD	1.29	<LOD	<LOD	<LOD	<LOD	<LOD	<LOD	<LOD	<LOD	<LOD
2020-07-08	<LOD	<LOD	<LOD	<LOD	<LOD	1.49	<LOD	<LOD	<LOD	<LOD	<LOD	<LOD	<LOD	<LOD	<LOD
2020-08-06	<LOD	<LOD	<LOD	<LOD	<LOD	0.26	<LOD	<LOD	<LOD	0.66	<LOD	<LOD	<LOD	<LOD	<LOD
2020-09-05	<LOD	<LOD	<LOD	<LOD	<LOD	0.81	<LOD	<LOD	<LOD	<LOD	<LOD	<LOD	<LOD	<LOD	<LOD
2020-10-03	<LOD	<LOD	<LOD	0.06	<LOD	0.24	<LOD	<LOD	<LOD	<LOD	<LOD	<LOD	<LOD	<LOD	<LOD
2020-11-01	<LOD	<LOD	<LOD	<LOD	<LOD	0.15	<LOD	<LOD	<LOD	<LOD	<LOD	<LOD	<LOD	<LOD	<LOD
LOD	0.21	0.07	0.05	0.04	0.58	0.05	0.50	0.09	0.17	0.27	33.61	0.002	0.04	0.01	0.004
LOQ	0.70	0.22	0.17	0.14	1.94	0.18	1.65	0.30	0.58	0.89	112.04	0.01	0.13	0.02	0.01
Tadoussac, QC															
2020-12-18	<LOD	<LOD	<LOD	<LOD	<LOD	<LOD	<LOD	<LOD	<LOD	<LOD	<LOD	<LOD	<LOD	<LOD	<LOD
2021-01-16	<LOD	<LOD	<LOD	<LOD	<LOD	<LOD	<LOD	<LOD	<LOD	<LOD	<LOD	<LOD	<LOD	<LOD	<LOD
2021-02-14	<LOD	<LOD	<LOD	<LOD	<LOD	<LOD	<LOD	<LOD	<LOD	<LOD	<LOD	<LOD	<LOD	<LOD	<LOD
2021-03-13	<LOD	<LOD	<LOD	<LOD	<LOD	<LOD	<LOD	<LOD	<LOD	<LOD	<LOD	<LOD	<LOD	<LOD	<LOD
2021-04-14	<LOD	<LOD	<LOD	<LOD	<LOD	<LOD	<LOD	<LOD	<LOD	<LOD	<LOD	<LOD	<LOD	<LOD	<LOD
2021-05-15	<LOD	<LOD	<LOD	<LOD	<LOD	<LOD	<LOD	<LOD	<LOD	<LOD	<LOD	<LOD	<LOD	<LOD	<LOD
2021-06-13	0.46	<LOD	<LOD	<LOD	<LOD	<LOD	<LOD	<LOD	<LOD	<LOD	<LOD	<LOD	<LOD	<LOD	<LOD
2021-07-12	<LOD	<LOD	<LOD	<LOD	<LOD	<LOD	<LOD	<LOD	<LOD	<LOD	<LOD	<LOD	<LOD	<LOD	<LOD
2021-08-10	<LOD	<LOD	<LOD	<LOD	<LOD	<LOD	<LOD	<LOD	<LOD	<LOD	<LOD	<LOD	<LOD	<LOD	<LOD
2021-09-08	<LOD	<LOD	<LOD	<LOD	<LOD	<LOD	<LOD	<LOD	<LOD	<LOD	<LOD	<LOD	<LOD	<LOD	<LOD
2021-10-07	<LOD	<LOD	<LOD	<LOD	<LOD	<LOD	<LOD	<LOD	<LOD	<LOD	<LOD	<LOD	<LOD	<LOD	<LOD
2021-11-05	<LOD	<LOD	<LOD	<LOD	<LOD	<LOD	<LOD	<LOD	<LOD	<LOD	<LOD	<LOD	<LOD	<LOD	<LOD
LOD	0.20	0.07	0.05	0.04	0.58	0.05	0.50	0.09	0.17	0.27	33.61	0.002	0.04	0.01	0.004
LOQ	0.65	0.22	0.17	0.14	1.94	0.18	1.65	0.30	0.58	0.89	112.04	0.01	0.13	0.02	0.01

Table S7 Concentrations, LODs, and LOQs of the polybrominated diphenyl ethers (PBDEs) in precipitation samples from Saturna Island, BC and Tadoussac, QC, in pg/L.

Start Date	PBDE congener concentration (pg/L)													
	17	28	49	66	71	85	99	100	138	153	154	183	190	209
Saturna Island, BC														
2019-12-18	<LOD	<LOD	<LOD	<LOD	<LOD	<LOD	<LOD	<LOD	<LOD	<LOD	<LOD	<LOD	<LOD	<LOD
2020-01-17	<LOD	<LOD	<LOD	<LOD	<LOD	<LOD	<LOD	8	<LOD	<LOD	<LOD	<LOD	<LOD	<LOD
2020-02-14	<LOD	<LOD	<LOD	<LOD	<LOD	<LOD	<LOD	<LOD	<LOD	<LOD	<LOD	<LOD	<LOD	<LOD
2020-03-15	<LOD	<LOD	<LOD	<LOD	<LOD	<LOD	<LOD	<LOD	<LOD	<LOD	<LOD	<LOD	<LOD	<LOD
2020-04-15	<LOD	<LOD	<LOD	<LOD	<LOD	<LOD	<LOD	<LOD	<LOD	<LOD	<LOD	<LOD	<LOD	<LOD
2020-05-11	<LOD	<LOD	<LOD	<LOD	<LOD	<LOD	<LOD	<LOD	<LOD	<LOD	<LOD	<LOD	<LOD	<LOD
2020-06-11	<LOD	<LOD	<LOD	<LOD	<LOD	<LOD	<LOD	<LOD	<LOD	<LOD	<LOD	<LOD	<LOD	<LOD
2020-07-08	<LOD	<LOD	<LOD	<LOD	<LOD	<LOD	<LOD	<LOD	<LOD	<LOD	<LOD	<LOD	<LOD	<LOD
2020-08-06	<LOD	<LOD	<LOD	<LOD	<LOD	<LOD	<LOD	<LOD	<LOD	<LOD	<LOD	<LOD	<LOD	<LOD
2020-09-05	<LOD	<LOD	<LOD	<LOD	<LOD	<LOD	<LOD	<LOD	<LOD	<LOD	<LOD	<LOD	<LOD	<LOD
2020-10-03	<LOD	<LOD	<LOD	<LOD	<LOD	<LOD	73	<LOD	<LOD	<LOD	<LOD	<LOD	<LOD	263
2020-11-01	<LOD	<LOD	<LOD	<LOD	<LOD	<LOD	69	<LOD	<LOD	25	<LOD	<LOD	<LOD	<LOD
LOD	0.7	0.7	4.6	5.2	5.1	11.7	10.0	1.9	13.1	9.4	5.7	10.7	22.6	47.0
LOQ	2.5	2.3	15.2	17.2	17.1	39.1	33.3	6.5	43.6	31.3	19.2	35.6	75.3	156.6
Tadoussac, QC														
2020-12-18	<LOD	<LOD	<LOD	<LOD	<LOD	<LOD	58	<LOD	<LOD	<LOD	8	<LOD	76	685
2021-01-16	<LOD	<LOD	<LOD	<LOD	<LOD	<LOD	57	<LOD	<LOD	<LOD	<LOD	<LOD	<LOD	219
2021-02-14	<LOD	<LOD	<LOD	<LOD	<LOD	<LOD	35	<LOD	<LOD	<LOD	<LOD	<LOD	<LOD	63
2021-03-13	<LOD	<LOD	<LOD	<LOD	<LOD	<LOD	<LOD	<LOD	<LOD	<LOD	<LOD	<LOD	77	655
2021-04-14	<LOD	<LOD	<LOD	<LOD	<LOD	<LOD	91	<LOD	<LOD	<LOD	<LOD	<LOD	<LOD	330
2021-05-15	<LOD	<LOD	<LOD	<LOD	<LOD	<LOD	118	<LOD	<LOD	<LOD	<LOD	<LOD	<LOD	403
2021-06-13	<LOD	<LOD	<LOD	<LOD	<LOD	<LOD	<LOD	<LOD	<LOD	<LOD	<LOD	<LOD	<LOD	92
2021-07-12	<LOD	<LOD	<LOD	<LOD	<LOD	<LOD	<LOD	<LOD	<LOD	<LOD	<LOD	<LOD	<LOD	131
2021-08-10	<LOD	<LOD	<LOD	<LOD	<LOD	<LOD	<LOD	<LOD	<LOD	<LOD	<LOD	<LOD	<LOD	108
2021-09-08	<LOD	<LOD	<LOD	<LOD	<LOD	<LOD	<LOD	<LOD	<LOD	<LOD	<LOD	<LOD	<LOD	138
2021-10-07	<LOD	<LOD	<LOD	<LOD	<LOD	<LOD	<LOD	<LOD	<LOD	<LOD	<LOD	<LOD	<LOD	117
LOD	2.2	4.5	4.3	7.5	4.5	8.2	24.2	7.6	17.6	17.0	3.9	5.0	42.0	17.0
LOQ	7.3	14.9	14.9	25.0	15.1	27.2	80.6	25.3	58.6	56.6	13.1	16.6	140.1	56.7

Table S8 Concentrations, LODs, and LOQs of the other brominated/halogenated flame retardants in precipitation samples from Saturna Island, BC and Tadoussac, QC, in pg/L.

Start Date	Concentration (pg/L)														
	ATE	**BATE**	**PBBz**	**PBT**	**PBEB**	**DBTE**	**HBBz**	**EHTBB**	**BTBPE**	**BEHTBP**	**DBDPE**	**Dec-602**	**Dec-604**	***syn*-DP**	***anti*-DP**
Saturna Island, BC															
2019-12-18	<LOD	<LOD	<LOD	<LOD	<LOD	<LOD	<LOD	<LOD	<LOD	<LOD	<LOD	<LOD	<LOD	306	<LOD
2020-01-17	<LOD	<LOD	<LOD	<LOD	<LOD	<LOD	<LOD	<LOD	<LOD	<LOD	<LOD	<LOD	<LOD	86	<LOD
2020-02-14	<LOD	<LOD	<LOD	<LOD	<LOD	<LOD	<LOD	<LOD	<LOD	<LOD	<LOD	<LOD	<LOD	21	<LOD
2020-03-15	<LOD	<LOD	<LOD	<LOD	<LOD	<LOD	<LOD	<LOD	<LOD	<LOD	<LOD	<LOD	<LOD	66	<LOD
2020-04-15	<LOD	<LOD	<LOD	<LOD	<LOD	<LOD	<LOD	<LOD	<LOD	<LOD	<LOD	<LOD	<LOD	30	<LOD
2020-05-11	<LOD	<LOD	<LOD	<LOD	<LOD	<LOD	<LOD	<LOD	<LOD	<LOD	<LOD	<LOD	<LOD	47	<LOD
2020-06-11	<LOD	<LOD	<LOD	<LOD	<LOD	<LOD	<LOD	<LOD	<LOD	<LOD	<LOD	<LOD	<LOD	39	<LOD
2020-07-08	<LOD	<LOD	<LOD	<LOD	<LOD	<LOD	<LOD	<LOD	<LOD	<LOD	<LOD	<LOD	<LOD	98	<LOD
2020-08-06	<LOD	<LOD	<LOD	<LOD	<LOD	<LOD	<LOD	<LOD	<LOD	<LOD	<LOD	<LOD	<LOD	<LOD	<LOD
2020-09-05	<LOD	<LOD	<LOD	<LOD	<LOD	<LOD	<LOD	<LOD	<LOD	<LOD	<LOD	<LOD	<LOD	59	<LOD
2020-10-03	<LOD	<LOD	<LOD	<LOD	<LOD	<LOD	<LOD	<LOD	<LOD	<LOD	<LOD	<LOD	<LOD	38	<LOD
2020-11-01	<LOD	<LOD	<LOD	<LOD	<LOD	<LOD	<LOD	<LOD	<LOD	<LOD	<LOD	<LOD	<LOD	37	<LOD
LOD	12.0	5.9	4.6	3.2	8.0	2.3	69.3	12.9	10.0	40.4	3683	0.6	4.5	1.4	0.9
LOQ	40.0	19.8	15.5	10.8	26.6	7.8	231.0	43.1	33.5	134.7	12275	2.0	15.1	4.7	3.0
Tadoussac, QC															
2020-12-18	<LOD	<LOD	<LOD	<LOD	<LOD	<LOD	<LOD	<LOD	<LOD	<LOD	<LOD	<LOD	<LOD	625	<LOD
2021-01-16	<LOD	<LOD	<LOD	<LOD	<LOD	<LOD	<LOD	<LOD	<LOD	<LOD	<LOD	<LOD	<LOD	134	<LOD
2021-02-14	<LOD	<LOD	<LOD	<LOD	<LOD	<LOD	<LOD	<LOD	<LOD	<LOD	<LOD	<LOD	<LOD	74	<LOD
2021-03-13	<LOD	<LOD	<LOD	<LOD	<LOD	<LOD	<LOD	<LOD	<LOD	<LOD	<LOD	<LOD	<LOD	211	<LOD
2021-04-14	<LOD	<LOD	<LOD	<LOD	<LOD	<LOD	<LOD	<LOD	<LOD	<LOD	<LOD	<LOD	<LOD	153	<LOD
2021-05-15	<LOD	<LOD	<LOD	<LOD	<LOD	<LOD	<LOD	<LOD	<LOD	<LOD	<LOD	<LOD	<LOD	86	<LOD
2021-06-13	<LOD	<LOD	<LOD	<LOD	<LOD	<LOD	<LOD	<LOD	<LOD	<LOD	<LOD	<LOD	<LOD	81	<LOD
2021-07-12	<LOD	<LOD	<LOD	<LOD	<LOD	<LOD	<LOD	<LOD	<LOD	<LOD	<LOD	<LOD	<LOD	233	<LOD
2021-08-10	<LOD	<LOD	<LOD	<LOD	<LOD	<LOD	<LOD	<LOD	<LOD	<LOD	<LOD	<LOD	<LOD	35	<LOD
2021-09-08	<LOD	<LOD	<LOD	<LOD	<LOD	<LOD	<LOD	<LOD	<LOD	<LOD	<LOD	<LOD	<LOD	42	<LOD
2021-10-07	<LOD	<LOD	<LOD	<LOD	<LOD	<LOD	<LOD	<LOD	<LOD	<LOD	<LOD	<LOD	<LOD	62	<LOD
LOD	14.3	4.1	3.2	2.3	5.6	1.6	48.3	9.0	7.0	28.2	2565	0.4	3.2	0.7	0.6
LOQ	47.7	13.8	10.8	7.5	18.6	5.5	160.9	30.0	23.3	93.8	8550	1.4	10.5	2.3	2.1

Text S2 Details on passive water sampling

At several sites passive water samplers (PWSs) were deployed at different depths, indicated as _Top, _Mid, and _Bot in Table S9. Duplicate measurements are labelled as _1, _2, etc. Before deployment, LDPE sheets were infused with a selected group of polycyclic aromatic hydrocarbons (d_{10}-acenaphthene, d_{10}-phenanthrene, d_{10}-pyrene, d_{12}-chrysene, d_{12}-indo[a,2,3-c,d] pyrene) and polychlorinated biphenyls (PCB-4, 9, 29, 62, 104, 127, 155, 184, and 204) as performance reference compounds (PRCs) to determine the sampling rates of the target analytes at each PWS site. The sheets were soaked in 1 L jars containing 800 mL of 4:1 methanol:water and the PRC solution in acetone, which were then equilibrated using a roller for five days at ambient temperature. The LDPE sheets were wiped with pre-extracted Kimwipes (dichloromethane (DCM) and acetone) to remove any residual water and methanol. Afterwards, the sheets were stored in an amber glass vial in a freezer until deployment.

Table S9 Deployment locations, dates, and lengths of the passive water samples, and the measured water concentrations in pg/L of TBECH and BDE-47 in BC and QC.

Site name	Latitude	Longitude	Deployment date	Retrieval date	Deployment length (d)	α-TBECH	β-TBECH	BDE-47
Quebec								
W1	45.534828	-73.527722	2021-07-28	2021-08-24	27	<LOD	<LOD	0.93
W2	45.565794	-73.509158	2021-07-28	2021-08-24	27	<LOD	<LOD	0.35
W3	45.734786	-73.417161	2021-07-28	2021-08-24	27	<LOD	<LOD	0.87
W4	45.790644	-73.344667	2021-07-28	2021-08-24	27	<LOD	<LOD	0.78
W5	46.041253	-73.164931	2021-07-28	2021-08-25	28	<LOD	<LOD	6.03
W6	46.243575	-72.745303	2021-07-29	2021-08-25	27	<LOD	<LOD	2.04
W7	46.3789	-72.446983	2021-07-29	2021-08-25	27	<LOD	<LOD	1.63
W8	46.832103	-71.171719	2021-07-30	2021-08-27	28	<LOD	<LOD	3.61
W9	46.844189	-71.171194	2021-07-30	2021-08-27	28	<LOD	<LOD	3.19
W10_1	48.507811	-68.517803	2021-04-29	2021-05-31	32	<LOD	<LOD	1.37
W10_2	48.507811	-68.517803	2021-04-29	2021-06-25	57	<LOD	<LOD	1.53
W10_3	48.507811	-68.517803	2021-04-29	2021-07-08	70	<LOD	<LOD	0.81
British Columbia								
V1_Top	49.29159	-122.88631	2021-06-21	2021-07-26	35	0.38	0.17	1.33
V1_Mid	49.29159	-122.88631	2021-06-21	2021-07-26	35	0.66	0.41	2.08
V1_Bot	49.29159	-122.88631	2021-06-21	2021-07-26	35	0.27	0.22	1.28
V2_1_Top	49.32041	-122.91019	2021-07-20	2021-08-09	20	0.08	<LOD	0.50
V2_1_Bot	49.32041	-122.91019	2021-07-20	2021-08-09	20	<LOD	<LOD	0.90
V2_2_Top	49.32041	-122.91019	2021-06-29	2021-07-20	21	<LOD	<LOD	1.11
V2_2_Bot	49.32041	-122.91019	2021-06-29	2021-07-26	27	0.07	<LOD	1.08
V3_1	49.33998	-123.2335	2021-05-14	2021-06-03	20	<LOD	<LOD	2.07
V3_2	49.33998	-123.2335	2021-05-14	2021-06-03	20	<LOD	<LOD	2.71
V3_3	49.33998	-123.2335	2021-05-14	2021-06-03	20	<LOD	<LOD	2.19
V4_1_Top	49.180346	-123.184825	2021-07-09	2021-07-30	21	<LOD	<LOD	1.05
V4_1_Mid	49.180346	-123.184825	2021-07-09	2021-07-30	21	0.08	<LOD	1.46
V4_1_Bot	49.180346	-123.184825	2021-07-09	2021-07-30	21	0.12	<LOD	0.95
V4_2_Top	49.180346	-123.184825	2021-07-30	2021-08-20	21	0.19	<LOD	1.36
V4_2_Mid	49.180346	-123.184825	2021-07-30	2021-08-20	21	0.36	0.3	1.49
V4_2_Bot	49.180346	-123.184825	2021-07-30	2021-08-20	21	0.21	0.09	1.49
V5_1_Top	49.08074	-123.130229	2021-06-24	2021-07-15	21	<LOD	<LOD	0.54
V5_1_Mid	49.08074	-123.130229	2021-06-24	2021-07-15	21	<LOD	<LOD	0.74
V5_1_Bot	49.08074	-123.130229	2021-06-24	2021-07-15	21	<LOD	<LOD	0.58
V5_2_Top	49.08074	-123.130229	2021-06-03	2021-06-24	21	0.12	<LOD	0.59

V5_2_Mid	49.08074	-123.130229	2021-06-03	2021-06-24	21	<LOD	<LOD	0.60
V5_2_Bot	49.08074	-123.130229	2021-06-03	2021-06-24	21	<LOD	<LOD	0.45
V6_Top	48.4381769	-123.381617	2021-08-10	2021-09-01	22	0.18	0.17	3.70
V6_Mid	48.4381769	-123.381617	2021-08-10	2021-09-01	22	0.19	0.11	2.13
V6_Bot	48.4381769	-123.381617	2021-08-10	2021-09-01	22	0.57	0.35	2.15
V7_Top	48.4274641	-123.3714434	2021-08-10	2021-09-01	22	0.36	0.3	2.05
V7_Bot	48.4274641	-123.3714434	2021-08-10	2021-09-01	22	0.44	0.33	1.46
V8_Top	48.4230709	-123.3712278	2021-08-10	2021-09-01	22	0.61	0.4	2.11
V8_Mid	48.4230709	-123.3712278	2021-08-10	2021-09-01	22	0.43	0.25	1.84
V8_Bot	48.4230709	-123.3712278	2021-08-10	2021-09-01	22	0.53	0.39	1.54
V9_Top	48.4235958	-123.3850258	2021-08-10	2021-09-01	22	0.62	0.43	0.88
V9_Mid	48.4235958	-123.3850258	2021-08-10	2021-09-01	22	0.74	0.62	1.19
V9_Bot	48.4235958	-123.3850258	2021-08-10	2021-09-01	22	0.89	0.56	0.99
V10_Top	48.4385813	-123.4336827	2021-08-10	2021-09-01	22	1.35	0.96	0.47
V10_Mid	48.4385813	-123.4336827	2021-08-10	2021-09-01	22	2.22	1.42	0.42
V10_Bot	48.4385813	-123.4336827	2021-08-10	2021-09-01	22	1.67	1.07	0.37

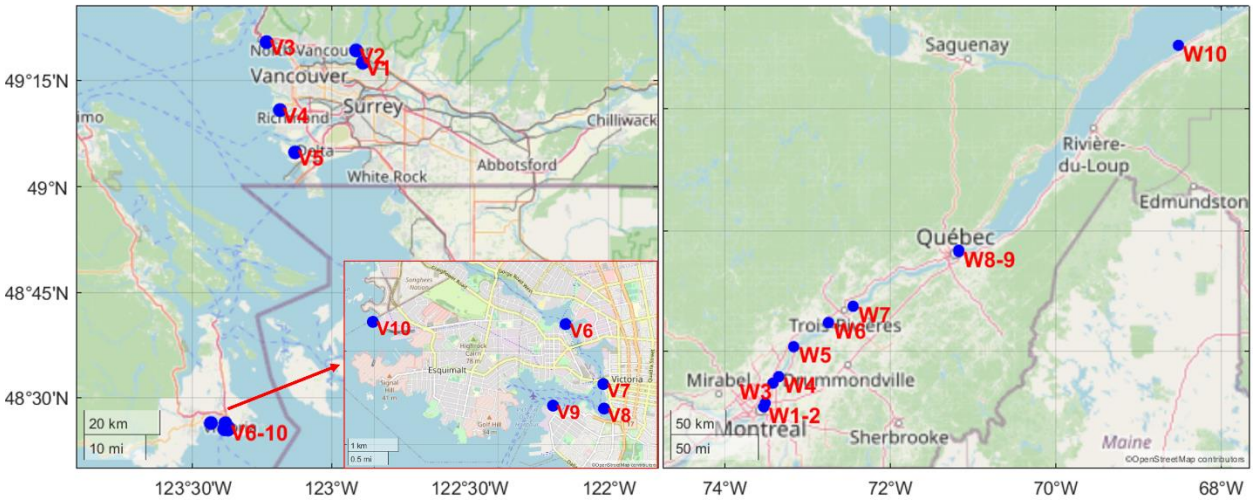

Figure S2 Map of the PWS sites and their site numbers in British Columbia (left) and Quebec (right).

Text S3 Details on sample extraction methods

Compounds were extracted from the XAD-2 resin (BC and QC PASs), the PUF/XAD-2/PUF sandwiches (Toronto AASs), and the GFFs (Saturna Island and Tadoussac AASs) by pressurised liquid extraction using an accelerated solvent extractor (ASE 350, Dionex, Sunnyvale, CA). Sample extraction was performed with hexane/acetone (V/V = 1:1) at 75°C and 1500 psi with a heat- and static-time of 6 min using three extraction cycles. The PUF/XAD-2/PUF sandwiches (Saturna Island and Tadoussac AASs) were Soxhlet extracted with 375 mL DCM for 20-22 hours. Compounds were extracted from the filtered precipitation samples using liquid-liquid extraction with 50 mL DCM three times. Compounds from the LDPE sheets were extracted by soaking in hexanes overnight two times. ^{13}C-labelled surrogates ($^{13}C_{12}$-BDE 28, $^{13}C_{12}$-BDE 47, $^{13}C_{12}$-BDE-99, $^{13}C_{12}$-BDE 139, $^{13}C_{12}$-BDE180, $^{13}C_{12}$-BDE209, $^{13}C_6$-PBBz, $^{13}C_6$-HBBz, $^{13}C_{10}$-Dec-602, $^{13}C_6$-EHTBB, $^{13}C_6$-BTBPE, $^{13}C_6$-BEHTBP, $^{13}C_{10}$-*anti*-DP, and $^{13}C_{14}$-DBDPE, were spiked into all samples prior to extraction. All extracts were reduced to 1 mL using a rotary evaporator and then passed through anhydrous sodium sulfate (baked at 450 °C overnight) to remove water residue. The extracts were

concentrated with high purity nitrogen and solvent-exchanged into iso-octane. The final volume of the extracts was ca. 0.5 mL. Injection standards ($^{13}C_{12}$-PCB-105, $^{13}C_{12}$-PCB-180, BDE-205, and $^{13}C_{10}$-Mirex) were added prior to instrumental analysis.

Text S4 Details on instrumental analysis and QA/QC procedures

Instrumental analysis for the quantification of these compounds in environmental samples was conducted by high-resolution gas chromatography (GC) coupled to TSQ8000 Evo triple quadrupole MS/MS equipped with a TriPlus RSH auto sampler, operated in EI mode. A volume of 2.0 µL was injected in pulsed splitless mode using a TriPlus RSH autosampler (80 ˚C for 0.05 min, followed by temperature ramp up to 280 ˚C at 14.5 ˚C/s). Chromatographic separation was accomplished using an RTX-5 column (Restek: 15 m, 0.25mm I.D., 0.1 µm film thickness) and helium as a carrier gas (flow rate: 1.2 mL/min). The ion source and interface temperature were set to 280 ˚C and 290 ˚C, respectively. The GC oven temperature program was set to begin at 90˚C, hold for 1 minute, ramp to 250˚C at 18 ˚C/min, then further ramp to 280 ˚C at 10 ˚C/min and finally, ramp to 310 ˚C at 30 ˚C/min and hold for 6 minutes. The precursor and product ions, as well as the collision energies (CEs) of the target compounds are tabulated in Table S10.

The air and passive water sample extracts were analyzed for enantiomers of α-TBECH using an Agilent 5977A mass spectrometer (MS) connected to a 7890B GC, with helium as the carrier gas at 1.2 mL min^{-1}. The GC- MS was operated in selected ion monitoring mode under negative chemical ionization mode. The chemical ionization reagent gas was methane. Enantiomers of α-TBECH were separated using a BGB-176MS column (10% 2,3-dimethyl-6-tert-butyldimethylsilyl-β-cyclodextrin in BGB 1, 15 m × 0.25 mm i.d., 0.18 µm film thickness, BGB Analytik AG, Switzerland) (Wong et al., 2012). The temperature of transfer line, inlet and ion source and quadrupole were at 250°C, 120°C and 150°C, respectively. The GC oven temperature was set at 80 °C for 1 min, then increased at a rate of 5 °C/min to 135 °C and held for 30 min and finally increased at a rate of 10 °C/min to 220 °C and held for 10 min. Splitless-mode injections of 2 µl were made using an autosampler/autoinjector system. The monitored ions were 79 and 81 m/z. To determine enantiomer fraction (EFs) for α-TBECH, the elution order was used and calculated as E1/(E1+E2), since the correspondence between optical signs and chromatographic elution is unknown for the TBECH (Wong et al., 2012).

Prior to use, all glassware was machine-washed (Miele) with detergent, rinsed with DI water, and baked for 24 hours. Laboratory equipment used to handle samples or extracts were cleaned and rinsed with acetone and hexane three times. The average recoveries of the ^{13}C-labeled HFRs whose native counterparts were detected in the samples in this study ($^{13}C_6$-PBBz, $^{13}C_{12}$-BDE-28, $^{13}C_{12}$-BDE-47, $^{13}C_{12}$-BDE-99, $^{13}C_{12}$-BDE-139, $^{13}C_{12}$-BDE-180, and $^{13}C_{12}$-BDE-209) are summarized in Table S11. Limits of detection (LOD) and quantification (LOQ) of each sampling technique were defined as the concentration at which the signal-to-noise ratio is equal to 3 and 10, respectively, and are tabulated for each target analyte in Table S12.

Blanks were used to quantify any contamination that may have occurred during preparation, transport, and handling of the samples. Procedural blanks (n=23) were clean collecting media that were not exposed to the environment, i.e., did not leave the laboratory. Field blanks are collecting media that underwent the same transport and processing as exposed samplers. PAS field blanks (BC: n=47; QC: n=19) consisted

of XAD-filled mesh cylinders that were briefly exposed to the air during the deployment of a PAS and then stored in a sealed shipping container at the sampling site for the duration of deployment. AAS field blanks (BC: n=6 QC: n=5; ON: n=4) were cartridges and GFFs that were briefly placed in the sampler without operating the pump. PWS field blanks (BC: n=10; QC: n=2) were LDPE sheets that were briefly exposed to the environment before being sealed and stored at the sampling site. Precipitation field blanks (BC: n=2 QC: n=3) were empty precipitation and overflow bottles briefly exposed to the environment before being sealed and stored at the sampling site for the duration of the employment. Blanks went through the entire extraction and quantification procedure with the samples. Levels of the analytes in all field and procedure blanks were consistently below LOD.

Table S10 The mass-to-charge ratios of precursor and product ions and the collision energies (CEs in eV) of the target halogenated flame retardants, internal standards, and injection standards.

Compound	Precursor	Product	CE
	329.8	140.8	40
ATE	331.8	142.9	30
	264.9	105.1	10
α-TBECH	266.9	105	10
	264.9	105.1	10
β-TBECH	266.9	105	10
	329.8	140.8	40
BATE	331.8	142.9	30
	471.5	311.8	50
PBBz	473.5	313.7	50
	480	319.7	45
$^{13}C_6$-PBBz	481.8	240.9	60
	245.9	139	35
BDE-17	405.8	246	20
	406.7	246.9	45
PBT	485.7	406.8	20
	245.9	139	35
BDE-28	405.8	245.9	20
	417.8	257.9	20
$^{13}C_{12}$-BDE-28	419.8	260	20
	335.9	265.9	15
$^{13}C_{12}$-PCB-105	337.9	267.9	15
	484.7	405.7	20
PBEB	499.7	484.7	20
	329.8	140.9	50
DPTE	331.8	142.9	50
	397.7	316.8	25
$^{13}C_6$-HBBz	477.6	397.7	30
	549.7	470.7	25
HBBz	551.8	391.6	50
	325.9	217	30
BDE-71	485.7	325.9	20
	325.9	217	30
BDE-49	485.7	325.9	20
	405.7	335.9	30
$^{13}C_{12}$-PCB-180	407.6	373	15
	325.9	217	30
BDE-47	485.7	325.9	20
$^{13}C_{12}$-BDE-47	337.9	148.9	55

Compound	Precursor	Product	CE
$^{13}C_6$-EHTBB	428.9	240.9	60
	444.9	321.9	60
$^{13}C_{12}$-BDE-99	575.6	415.7	26
	575.6	417.7	26
EHTBB	422.8	313.8	40
	422.8	394.7	25
BDE-85	403.8	296.8	35
	565.7	405.9	25
BDE-154	483.7	323.8	50
	643.7	483.4	25
BDE-153	483.7	323.8	50
	643.7	483.4	25
$^{13}C_{12}$-BDE-139	497.7	228	60
	655.7	495.7	40
BDE-138	483.7	323.8	50
	643.7	483.4	25
Dec-604	417.8	338.8	15
	419.8	259.9	25
BDE-183	561.7	454.5	50
	721.7	561.7	25
BTBPE	356.8	251.9	25
	358.8	251.9	30
$^{13}C_6$-BTBPE	362.8	95.1	55
	364.8	283.9	10
$^{13}C_{12}$-BDE-180	573.7	413.8	45
	575.7	415.8	45
BDE-190	561.7	454.5	50
	721.7	561.7	25
$^{13}C_6$-BEHTBP	128.3	62.1	15
	128.3	80.5	5
BEHTBP	462.7	378.7	40
	464.7	380.7	40
syn-DP	273.6	238.8	25
	271.8	236.9	25
anti-DP	271.8	236.9	25
	273.6	238.8	25
$^{13}C_{10}$-*anti*-DP	277	242	25
	279	244	25
BDE-205	641.7	534.5	50

	497.7	337.9	25
	325.9	217	30
BDE-66	485.7	325.9	20
$^{13}C_8$-Mirex	275.7	240.6	30
	403.8	296.8	35
BDE-100	565.7	405.9	25
	271.8	236.9	20
Dec-602	273.6	238.9	20
$^{13}C_{10}$-Dec-602	277	242	20
	403.8	296.8	35
BDE-99	565.7	405.9	25

	801.7	641.7	25
	801.7	641.7	50
BDE-209	799.7	639.8	50
	959.4	799.3	32
$^{13}C_{12}$-BDE-209	811.8	651.4	45
	971.4	811.3	32
DBDPE	484.7	324.7	60
	486.7	326.7	50
$^{13}C_{14}$-DBDPE	491.7	331.8	60
	493.6	333.9	60

Table S11 Summary of the recoveries of the ^{13}C-labeled HFRs from the samples of this study.

Compound	Recovery (%)			
	PAS	AAS	Precipitation	PWS
$^{13}C_6$-PBBz	102.2±20.2	84.7±21.9	88.0±16.1	107.0±9.3
$^{13}C_{12}$-BDE-28	106.7±22.5	89.1±24.5	85.7±12.9	94.5±6.1
$^{13}C_{12}$-BDE-47	120.2±11.2	107.0±39.6	97.1±13.1	106.0±6.8
$^{13}C_{12}$-BDE-99	117.4±15.5	98.3±39.4	103.0±16.6	104.8±8.0
$^{13}C_{12}$-BDE-139	145.1±32.8	156.5±84.3	139.5±39.3	141.7±38.1
$^{13}C_{12}$-BDE-180	170.7±46.6	182.5±114.0	152.8±53.7	159.7±26.2
$^{13}C_{12}$-BDE-209	138.7±45.7	114.8±84.5	168.3±90.4	245.5±91.6

Table S12 The average LOD and LOQ of TBECH and BDE-47 from the passive air sampling and passive water sampling network, as well as the precipitation samples and AAS stations. All volumetric air and water concentrations are expressed in pg/m^3 and pg/L, respectively.

		α-TBECH	β-TBECH	BDE-47
PAS network	LOD	0.10	0.13	0.59
	LOQ	0.33	0.43	2.00
PWS network	LOD	0.06	0.05	0.02
	LOQ	0.20	0.17	0.068
Saturna Island, BC AAS	LOD	7.17×10^{-3}	7.17×10^{-3}	0.07
	LOQ	0.02	0.02	0.24
Saturna Island, BC precipitation bottles	LOD	0.2	0.2	0.4
	LOQ	0.6	0.6	1.3
Tadoussac, QC AAS	LOD	7.17×10^{-3}	7.17×10^{-3}	0.046
	LOQ	0.02	0.02	0.15
Tadoussac, QC precipitation bottles	LOD	2.9	3.9	12.4
	LOQ	9.8	13.2	41.5
Toronto, ON AAS	LOD	0.01	0.01	0.02
	LOQ	0.04	0.04	0.05

Text S5 Details on calculation of air and water concentrations

Volumetric air concentrations were calculated by dividing the amount of a target compound quantified in a PAS (pg) by the product of a sampling rate in m^3/day and the deployment period in days. The sampling rates of α- and β-TBECH and BDE-47 were 0.41, 0.35, and 0.17 m^3/day, respectively (Li et al., 2023). Water concentrations of the target analytes were calculated by using the retained fraction (f) of the PRCs in the deployed LDPE sheets. Using a spreadsheet provided by Booij and Smedes (2010) (Excel Solver add-in), a

nonlinear least squares (NLS) estimation was used to determine a site- and compound specific sampling rate (R_s is in L/d) and a site-specific coefficient (FA) with the following equations:

$$f = exp[(-R_S t)/(K_{PW} m_P)] \quad \text{(eq1)}$$

$$R_S = FA\ M^{-0.35} \quad \text{(eq2)}$$

where t is the deployment time (days), K_{PW} is the LDPE PWS-water partition ratio (L/kg), m_P is the average mass of the LDPE sheets (kg), M is the molecular weight of the compound (g/mol). K_{PW} values of the target analytes were estimated with calculated Abraham solute descriptors (Ulrich et al., 2017) using the models detailed in Khawar and Nabi (2021). K_{PW} values of the PRCs were derived using the solvation models by Smedes et al. (2009). Once the FA values of each site were estimated using the PRC dissipation data, R_s was adjusted to each analyte using equation 2. The volumetric water concentration (C_w) of each analyte was then calculated:

$$C_W = \frac{N}{K_{PW} m_P \left[1 - exp\left({}^{-R_S t}/_{K_{PW} m_P}\right)\right]} \quad \text{(eq3)}$$

where N is the amount of target analyte accumulated on the LDPE sheets.

Text S6 Details on COSMOtherm predictions

Equilibrium partition ratios between octanol and water (K_{ow}), octanol and air (K_{oa}), and air and water (K_{aw}) were estimated with the Conductor like Screening Model for Realistic Solvents (COSMO-RS) software suite. The COSMO-RS is a chemical property prediction tool, which requires both COSMOconf with TURBOMOLE and COSMOtherm from Dassault Systèmes. This approach uses both quantum chemical density functional theory (DFT) and statistical thermodynamics of the molecular interactions to predict various physical-chemical properties of compounds. Using COSMO-RS consists of two parts, with the first part involving the use of COSMOconf with TURBOMOLE to determine different possible conformations of the molecule based on its polar charge density and how these charges interact with a virtual conductor environment using DFT/COSMO calculations. The resulting electron density and geometry of the molecule are used to identify the most energetically optimal state for the compound in the virtual conductor (Klamt et al., 2009). For the second part, COSMOtherm is then used to quantify the interaction energy of the chemical in two different phases by using the polar charge density of the different conformations of the compound. When combined with statistical thermodynamics, the chemical potential of the compound in the different phases, and therefore, the Gibbs free energy of the phase transfer (ΔG°) can be calculated (Klamt et al., 2009), which can be converted into partition ratios using the following equation:

$$Log\ K = Log\left(exp\left(\frac{-\Delta G^{\circ}}{RT}\right)\right)$$

The SDF text files of the isomers, generated by OpenBabel v3.11, were entered into COSMOconf v20.0.0 with TURBOMOLE v4.5 to generate COSMO files. All conformers were entered into COSMOtherm v20.0.0 using the TZVPD-FINE parameterization to calculate the ΔG° for each isomer at a given temperature, which were then converted into its corresponding log K values.

Table S13 Comparison of the mean/median and range of the air concentrations of α- and β-TBECH reported in this study, with those reported in previous studies, categorized by the type of sampling location (outdoor air vs. indoor air and urban vs. remote regions).

Location	n=	Date	Sampling technique	Concentration in pg m^{-3} average (A) or median (M) (Range)		α/β-ratio	ref.
Outdoor Air in Source Regions				α	β		
Stockholm, Sweden	24	Apr 2014–May 2015	AAS (GFF, 2 PUFs)	0.52 (M) (0.13–1.2)	0.35 (M) (0.11–0.88)	1.5	(Wong et al., 2018)
Stockholm, Sweden	28	Apr–Jun 2012	AAS (GFF, 2 PUFs)	0.36 (M) (<0.087–1.4)	0.20 (M) (<0.079–0.95)	1.8	(Newton et al., 2015)
Birmingham, UK	48	Jun 2012–Jan 2013	PAS (PUF, GFF)	2.2 (M) (<0.078–28)	1.7 (M) (<0.063–15)	1.3	(Drage et al., 2016)
Ziya Town, China	1	Jun–Aug 2011	PAS (PUF)	9.0	30	0.30[b]	(Hong et al., 2018)
Brno, Czech Republic	17	July–Aug 2010	PAS (PUF)	Σα,β,γ,δ: 7.8 (M) (1.7–1500)		N/A	(Melymuk et al., 2016)
	20	Feb–Mar 2011		Σα,β,γ,δ: 0.75 (M) (0.85–1.2)		N/A	
Toronto, Canada	70	Mar 2010–Apr 2011	AAS (GFF, PUF/XAD/PUF)	N/A	2.9 (M) (<0.41–7.22)	N/A	(Shoeib et al., 2014)
Brno, Czech Republic	36	Sep–Dec 2010	PAS (PUF)	Σα,β,γ,δ: 2.76 (A)		N/A	(Bohlin et al., 2014)
Lhasa, Tibet	84	Aug 2008–July 2010	AAS (GFF, PUF)	Σα,β,γ,δ: 1.9 (A) (ND-10)		N/A	(Ma et al., 2017)
Toronto, Ontario	48	Jun 2020–May 2021	AAS (GFF, PUF/XAD/PUF)	0.40 (A) (0.18–1.34)	0.26 (A) (0.11–0.87)	1.5	this study
72 sites in Quebec	86	Nov 2019–May 2022	PAS (XAD)	0.22 (A) (<0.10–1.21)	0.22 (A) (<0.13–0.99)	1.0	
46 sites in BC	78	Jan 2020–Apr 2022	PAS (XAD)	0.54 (A) (<0.10–2.22)	0.46 (A) (<0.13–2.11)	1.2	
Outdoor air in remote regions							
Saturna Island, BC	11	Dec 2019–Nov 2020	AAS (GFF, PUF/XAD/PUF)	0.07 (A) (ND–0.14)	0.03 (A) (ND–0.12)	2.3	this study
Tadoussac, QC	12	Dec 2020–Nov 2021	AAS (GFF, PUF/XAD/PUF)	0.13 (A) (ND–0.29)	0.08 (A) (ND–0.17)	1.5	
King George Island, Antarctica	N/A	2011–2018	AAS (GFF, PUF)	(ND–0.39)	(ND–0.21)	ND-1.9	(Zhao et al., 2020)
Longyearbyen, Svalbard[a]	3	2015–2017	PAS (Silicone rubber)	48 (A) (29–65)	31 (B) (17–46)	1.6	(Carlsson et al., 2018)
Indoor Air							
Stockholm, Sweden, Office	23	Apr 2014–May 2015	AAS (GFF, 2 PUFs)	13 (M) (7.4–22)	8.5 (M) (5.8–16)	1.5	(Wong et al., 2018)
Offices, homes, stores, schools	48	Feb–May 2012	AAS (GFF, 2 PUFs)	36 (M) (<3.5–510)	19 (M) (<2.8–270)	1.9	(Newton et al., 2015)
Birmingham, UK, Homes	15	Feb–May 2015	PAS (PUF, GFF)	99 (A) (17–350)	74 (A) (13–250)	1.3	(Tao et al., 2016)
Offices	20			180 (A) (74–440)	140 (A) (41–300)	1.3	
Computer repair, Izmir, Turkey	15	Mar–Jun 2016	PAS & AAS (PUF)	564 (A)	375 (A)	1.5	(Genisoglu et al., 2019)
Brno, Czech Republic, Homes	17	July–Aug 2010	PAS (PUF)	Σα,β,γ,δ: 32 (M) (6.5–1900)		N/A	(Melymuk et al., 2016)
	20	Feb–Mar 2011		Σα,β,γ,δ: 20 (M) (7.7–530)		N/A	
Oslo, Norway, Living rooms	47	Jan–May 2012	AAS (Quartz filter, PUF)	Σα,β: 222 (A) (77.9–4120)		N/A	(Cequier et al., 2014)
Classrooms	6			Σα,β: 104 (A) (104–399)		N/A	
Beijing, China, Offices,	36	Spring-summer 2013	PAS, AAS (GFF, PUF)	Σα,β: (<0.16–82)		N/A	(Newton et al., 2016)

[a] The concentrations reported for the sampling site in Longyearbyen, Svalbard, are two to three orders of magnitude higher than at the other two remote sampling sites and two order of magnitudes higher than most urban sites. This has been attributed to a local unidentified source (Carlsson et al., 2018).

[b] The measurement at the electronic waste processing site in China is the only one that reports a higher abundance of β-TBECH than α-TBECH. The high temperatures involved with e-waste dismantling may potentially have skewed the ratio through thermal interconversion (Arsenault et al., 2008).

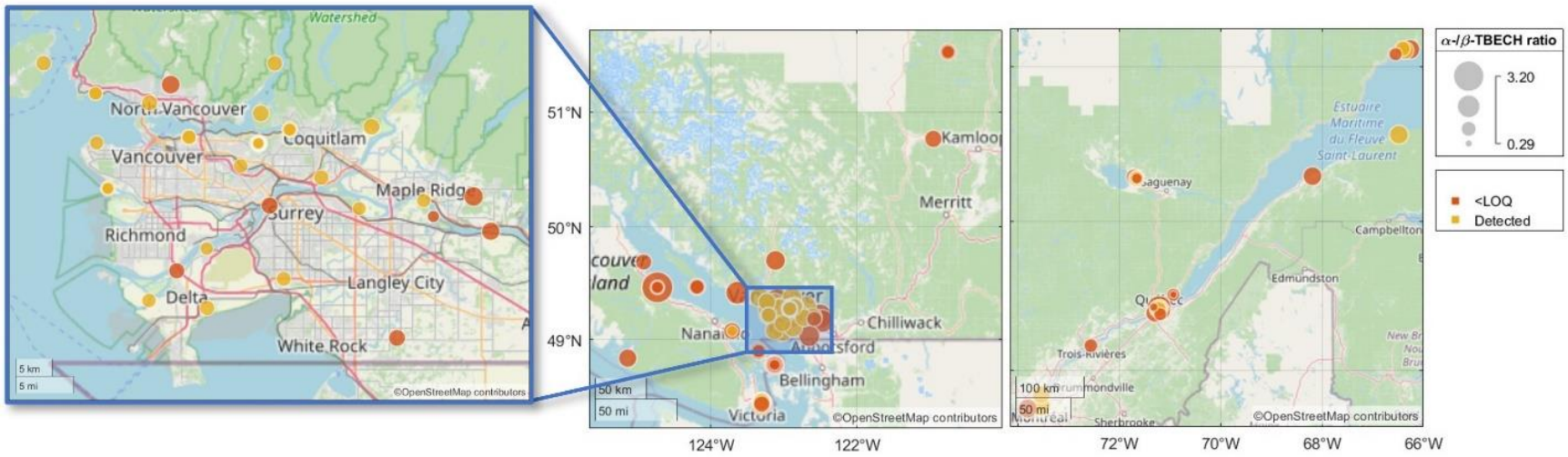

Figure S3 The spatial distribution of the atmospheric α-/β-TBECH ratios in the PAS sites in British Columbia (middle) and Quebec (right). A close-up map of the Vancouver metropolitan area of British Columbia is shown (left) for a detailed view of the clustered sites. To calculate the ratio, only measurements that were the LOD of both isomers were used, including measurements that were above the LOD but below the LOQ. TBECH concentrations with at least one isomer below the LOQ are marked on the map as <LOQ.

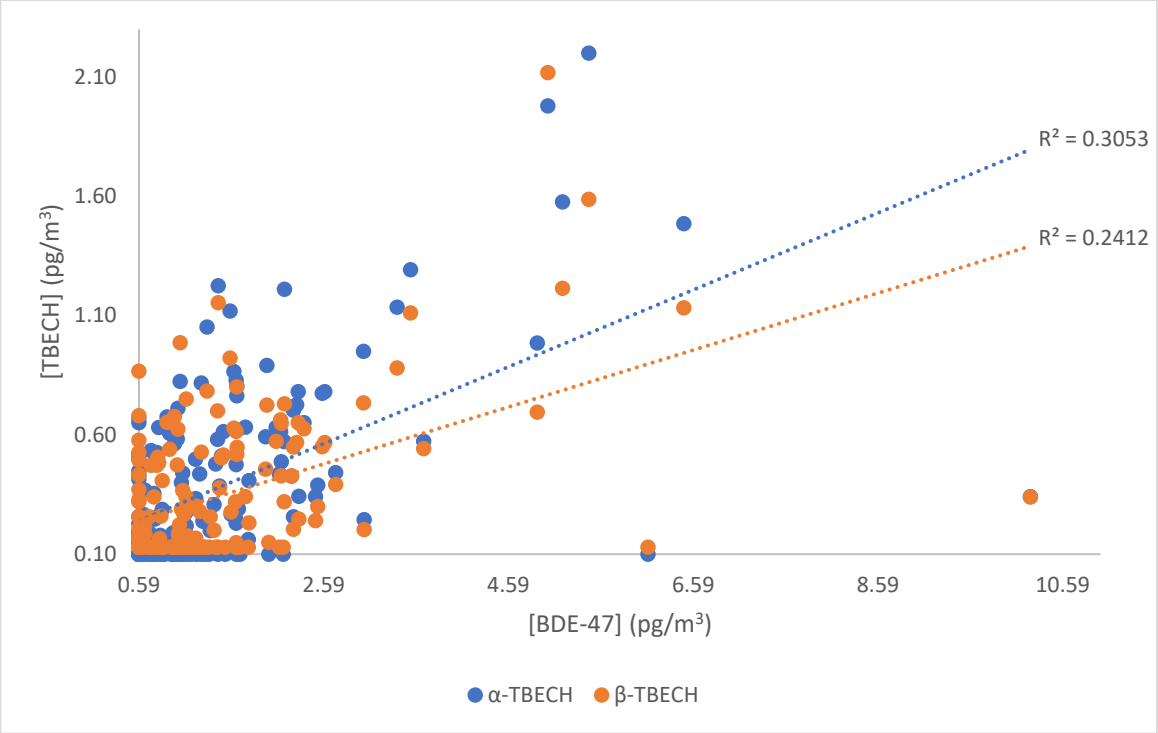

Figure S4 The relationship between the air concentration of α- and β-TBECH and BDE-47 in the British Columbia and Quebec PAS sites. Air concentration measurements of the chemicals that were below the LOD were given a value of the LOD when plotted.

Table S14 The linear regression parameters for Figure S4.

		Coefficient	Std. error	*t*	*P*	(Adjusted) R^2	Significance F
α-TBECH	Intercept	0.15	0.036	4.07	<0.0001	(0.30) 0.31	<0.0001
	x-variable	0.16	0.019	8.57	<0.0001		
β-TBECH	Intercept	0.17	0.031	5.44	<0.0001	(0.24) 0.24	<0.0001
	x-variable	0.12	0.016	7.29	<0.0001		

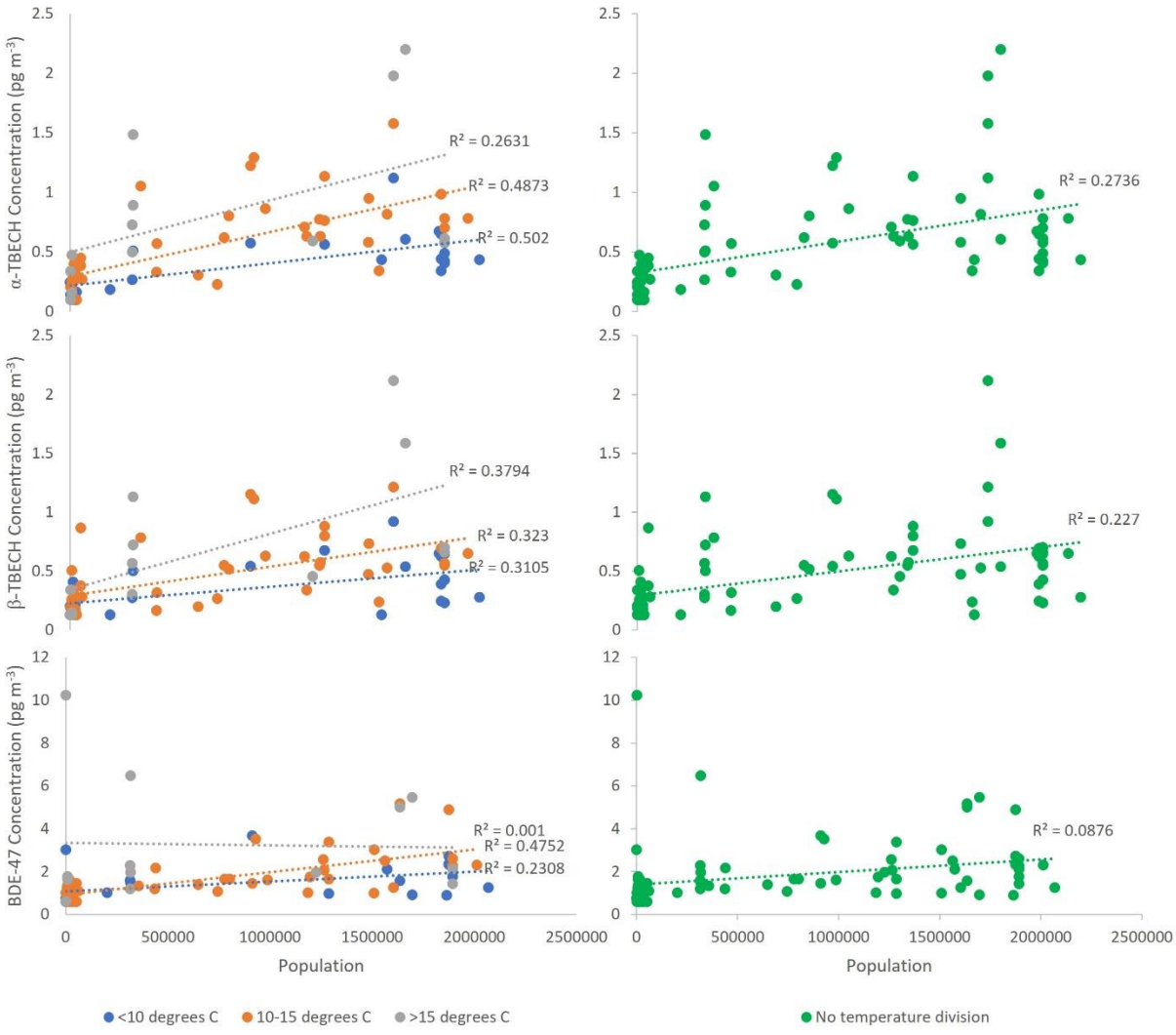

Figure S5 The relationship between the air concentration of α-TBECH (top), β-TBECH (middle), and BDE-47 (bottom) in the British Columbia PAS sites and the population in a 20-km radius around the sites. Sites were divided based on the average air temperature during their deployment length (left) and compared to the overall sample set (right) for each chemical.

Table S15 The linear regression parameters for Figure S5

		Coefficient	Std. error	*t*	*P*	(Adjusted) R^2	Significance F
All sampling seasons (x-variable: population; y-variable: volumetric concentration; n=83)							
α-TBECH	Intercept	0.32	0.056	5.82	<0.0001	(0.26) 0.27	<0.0001
	x-variable	2.80×10^{-7}	5.07×10^{-8}	5.52	<0.0001		
β-TBECH	Intercept	0.29	0.049	5.98	<0.0001	(0.22) 0.23	<0.0001
	x-variable	2.18×10^{-7}	4.48×10^{-8}	4.88	<0.0001		
BDE-47	Intercept	1.40	0.23	6.11	<0.0001	(0.076) 0.088	0.0066
	x-variable	5.84×10^{-7}	2.09×10^{-7}	2.79	0.0066		
<10°C (x-variable: population; y-variable: volumetric concentration; n=27)							
α-TBECH	Intercept	0.22	0.047	4.64	<0.0001	(0.48) 0.50	<0.0001
	x-variable	1.86×10^{-7}	3.70×10^{-8}	5.02	<0.0001		
β-TBECH	Intercept	0.23	0.052	4.36	0.00020	(0.28) 0.31	0.0025
	x-variable	1.38×10^{-7}	4.13×10^{-8}	3.36	0.0025		
BDE-47	Intercept	1.07	0.22	4.95	<0.0001	(0.20) 0.23	0.011
	x-variable	4.67×10^{-7}	1.70×10^{-7}	2.74	0.011		
10-15°C (x-variable: population; y-variable: volumetric concentration; n=43)							
α-TBECH	Intercept	0.29	0.058	5.06	<0.0001	(0.47) 0.49	<0.0001
	x-variable	3.69×10^{-7}	5.91×10^{-8}	6.24	<0.0001		
β-TBECH	Intercept	0.29	0.054	5.44	<0.0001	(0.31) 0.32	<0.0001
	x-variable	2.42×10^{-7}	5.47×10^{-8}	4.42	<0.0001		
BDE-47	Intercept	0.92	0.17	5.35	<0.0001	(0.46) 0.48	<0.0001
	x-variable	1.06×10^{-6}	1.74×10^{-7}	6.09	<0.0001		
>15°C (x-variable: population; y-variable: volumetric concentration; n=13)							
α-TBECH	Intercept	0.50	0.23	2.18	0.052	(0.20) 0.26	0.073
	x-variable	4.30×10^{-7}	2.17×10^{-7}	1.98	0.073		
β-TBECH	Intercept	0.35	0.19	1.81	0.097	(0.32) 0.38	0.025
	x-variable	4.67×10^{-7}	1.80×10^{-7}	2.59	0.025		
BDE-47	Intercept	3.33	1.12	2.97	0.013	(-0.090) 0.001	0.92
	x-variable	-1.10×10^{-7}	1.06×10^{-6}	-0.11	0.92		
Two x-variables: population in 20-km radius and 1/AAT; y-variable: Ln(P); n=83							
α-TBECH	Intercept	-3.27	4.41	-0.74	0.46	(0.56) 0.57	<0.0001
	x-variable 1 (population)	6.92×10^{-7}	7.30×10^{-8}	9.47	<0.0001		
	x-variable 2 (1/AAT)	-6860.43	1260.51	-5.44	<0.0001		
β-TBECH	Intercept	-8.13	4.78	-1.70	0.093	(0.42) 0.43	<0.0001
	x-variable 1 (population)	5.82×10^{-7}	7.91×10^{-8}	7.35	<0.0001		
	x-variable 2 (1/AAT)	-5489.59	1365.92	-4.02	0.00013		
BDE-47	Intercept	-9.23	4.54	-2.03	0.045	(0.34) 0.36	<0.0001
	x-variable 1 (population)	4.59×10^{-7}	7.52×10^{-8}	6.11	<0.0001		
	x-variable 2 (1/AAT)	-4782.41	1297.21	-3.69	0.00041		

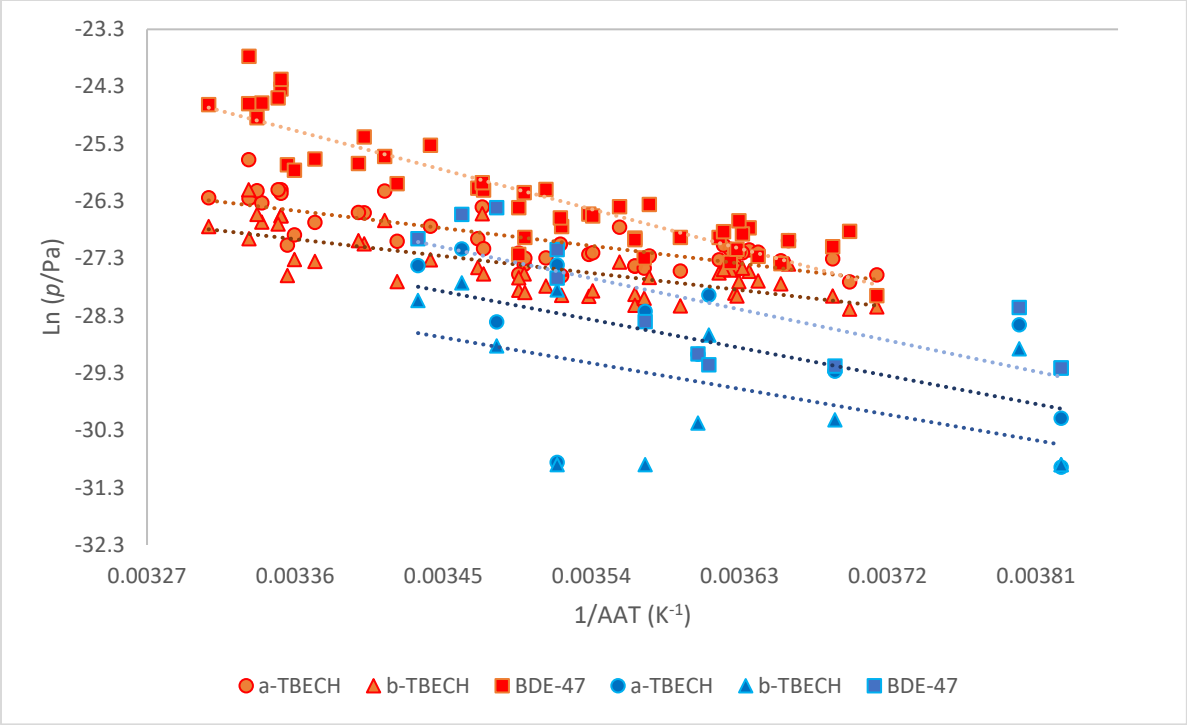

Figure S6 The temperature dependence of the air concentrations of α-TBECH (circle), β-TBECH (triangle), and BDE-47 (square) in Scarborough, ON (orange) and Tadoussac, QC (blue).

Table S16 The linear regression parameters for Figure S6

		Coefficient	Std. error	*t*	*P*	(Adjusted) R^2	Significance F
Toronto, ON (single x-variable: 1/AAT; y-variable: Ln(P); n=48)							
α-TBECH	Intercept	-15.01	1.39	-10.80	<0.0001	(0.61) 0.61	<0.0001
	x-variable	-3408.32	395.93	-8.61	<0.0001		
β-TBECH	Intercept	-15.93	1.53	-10.38	<0.0001	(0.54) 0.55	<0.0001
	x-variable	-3283.00	437.06	-7.512	<0.0001		
BDE-47	Intercept	0.53	1.91	0.28	0.78	(0.81) 0.81	<0.0001
	x-variable	-7618.84	545.15	-13.98	<0.0001		
Saturna Island, BC (x-variable: 1/AAT; y-variable: Ln(P); n=11)							
α-TBECH	Intercept	-28.58	20.85	-1.37	0.20	(-0.11) <0.0001	0.98
	x-variable	-128.00	5909.27	-0.022	0.98		
β-TBECH	Intercept	-19.72	19.06	-1.03	0.33	(-0.08) 0.03	0.61
	x-variable	-2847.55	5404.12	-0.53	0.61		
BDE-47	Intercept	1.74	10.83	0.16	0.88	(0.37) 0.44	0.027
	x-variable	-8114.23	3069.38	-2.64	0.027		
Tadoussac, QC (x-variable: 1/AAT ; y-variable: Ln(P); n=12)							
α-TBECH	Intercept	-9.08	8.44	-1.08	0.31	(0.29) 0.35	0.042
	x-variable	-5447.27	2334.11	-2.33	0.042		
β-TBECH	Intercept	-11.49	8.67	-1.33	0.21	(0.23) 0.30	0.064
	x-variable	-4982.64	2398.45	-2.08	0.064		
BDE-47	Intercept	-6.33	5.56	-1.14	0.28	(0.57) 0.60	0.003
	x-variable	-6020.33	1538.73	-3.91	0.003		

Text S7 Investigating the influence of wind on the concentrations of BFRs measured during active air sampling (AAS) in Toronto

Hourly wind direction and speed measurements were provided by the University of Toronto Scarborough during each sampling period. Each wind direction measurement was divided into three categories: originated from rural areas (rural winds), originated from Lake Ontario (lake winds), and originated from the Toronto urban centre (urban winds), which are shown in Figure S7. In this study, an urban wind fraction UWF is defined as a fraction of the number of wind direction measurements originating from the Toronto urban centre over the total number of wind measurements in the sampling period.

To investigate whether the wind originating from the Toronto urban centre was a factor affecting the concentration of the BFRs, the logarithm of the partial pressure ln(P) α- and β-TBECH and BDE-47 was regressed with UWF and reciprocal air temperature (Table S17).

Figure S7 The population density map of the Greater Toronto Area (GTA) with the detailed division of the wind origin arriving at Scarborough, ON, centered at the AAS station. Population density map was provided by CensusMapper, using data released by Statistics Canada.

Table S17 Multiple linear regression parameters for relationships between the logarithm of the partial pressure of a BFR in Toronto, ON (ln(*p*/Pa), and reciprocal temperature (1/AAT) and a wind fraction (XWF, X=U Urban, R Rural, L Lake). Number of datapoints is 48.

		Coefficient	**Std. error**	***t***	***P***	**(Adjusted) R^2**	**Significance F**
Urban Wind Fraction (UWF)							
α-TBECH	Intercept	-14.75	1.28	-11.52	<0.0001	(0.67) 0.68	<0.0001
	1/AAT	-3547.00	366.74	-9.67	<0.0001		
	UWF/speed	7.05	2.29	3.07	0.0036		
β-TBECH	Intercept	-15.58	1.35	-11.56	<0.0001	(0.65) 0.66	<0.0001
	1/AAT	-3466.18	386.07	-8.98	<0.0001		
	UWF/speed	9.31	2.42	3.85	0.00037		
BDE-47	Intercept	0.71	1.90	0.37	0.71	(0.81) 0.82	<0.0001
	1/AAT	-7710.29	544.24	-14.17	<0.0001		
	UWF/speed	4.65	3.41	1.37	0.18		
Rural Wind Fraction (RWF)							
α-TBECH	Intercept	-15.02	1.40	-10.74	<0.0001	(0.60) 0.62	<0.0001
	1/AAT	-3434.86	400.11	-8.58	<0.0001		
	RWF/speed	1.36	1.99	0.68	0.50		
β-TBECH	Intercept	-15.93	1.55	-10.28	<0.0001	(0.53) 0.55	<0.0001
	1/AAT	-3293.32	443.69	-7.42	<0.0001		
	RWF/speed	0.53	2.21	0.24	0.81		
BDE-47	Intercept	0.53	1.93	0.28	0.78	(0.81) 0.80	<0.0001
	1/AAT	-7598.10	552.85	-13.74	<0.0001		
	RWF/speed	-1.07	2.75	-0.39	0.70		
Lake Wind Fraction (LWF)							
α-TBECH	Intercept	-14.52	1.75	-8.28	<0.0001	(0.60) 0.61	<0.0001
	1/AAT	-3536.22	483.68	-7.31	<0.0001		
	LWF/speed	-0.75	1.60	-0.47	0.64		
β-TBECH	Intercept	-16.69	1.93	-8.65	<0.0001	(0.53) 0.56	<0.0001
	1/AAT	-3085.13	532.67	-5.79	<0.0001		
	LWF/speed	1.16	1.76	0.66	0.51		
BDE-47	Intercept	0.90	2.42	0.37	0.71	(0.81) 0.80	<0.0001
	1/AAT	-7714.83	667.11	-11.56	<0.0001		
	LWF/speed	-0.56	2.20	-0.26	0.80		

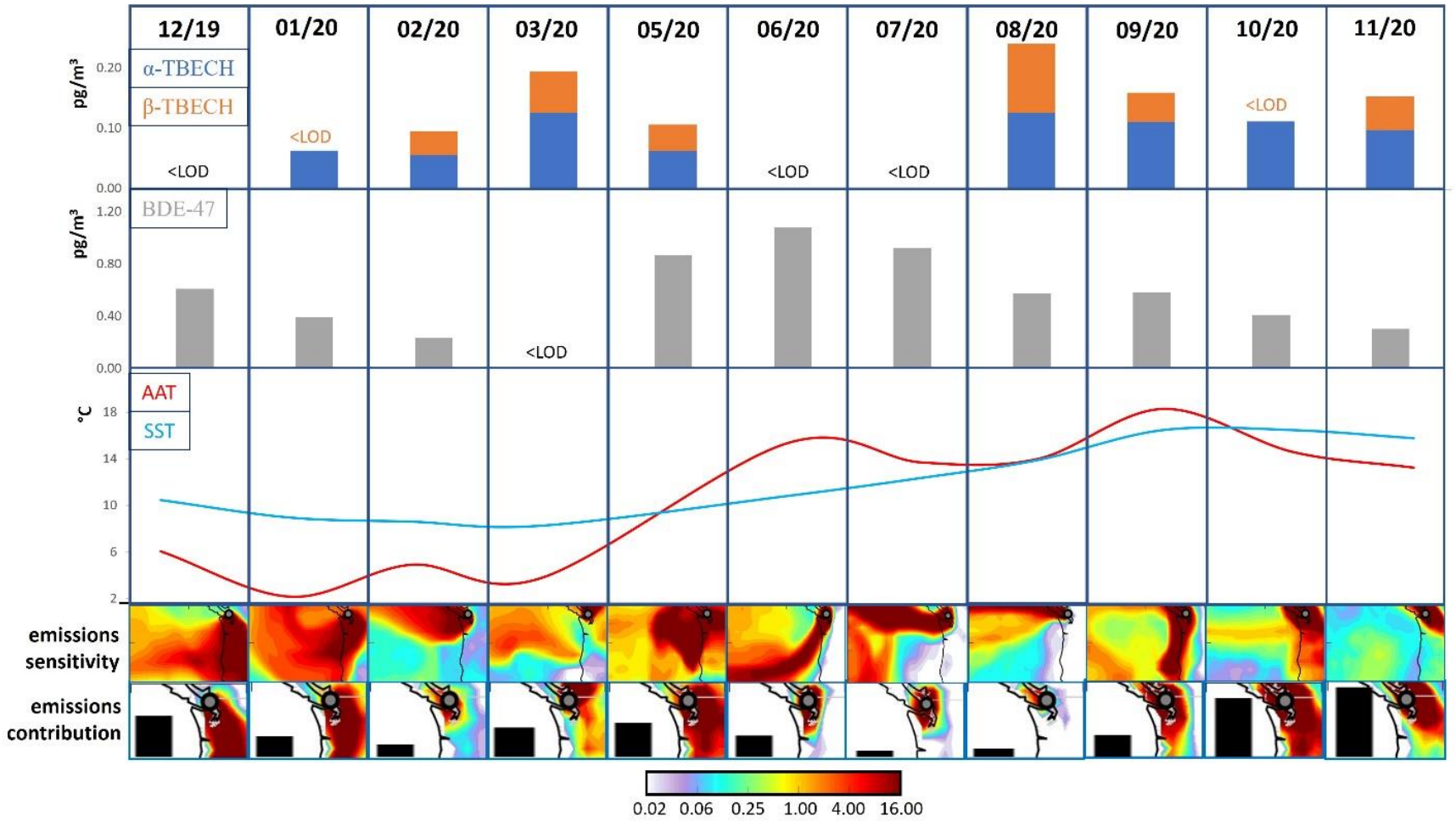

Figure S8 Air concentration (gas phase only) of α- and β-TBECH (stacked) and BDE-47 on Saturna Island, BC (top) and the average surface sea (SST) and air temperature (AAT) taken during each sampling period (middle). The maps of FLEXPART (bottom) show the emissions sensitivity (ES) and emissions contribution (EC) of the BC region during each sampling period, with units of ns m^{-2} and ng m^{-3} m^{-2}, respectively. The black bars overlayed on the EC FLEXPART maps indicate the relative model-predicted average air concentration of CO at the measurement site during the sampling period.

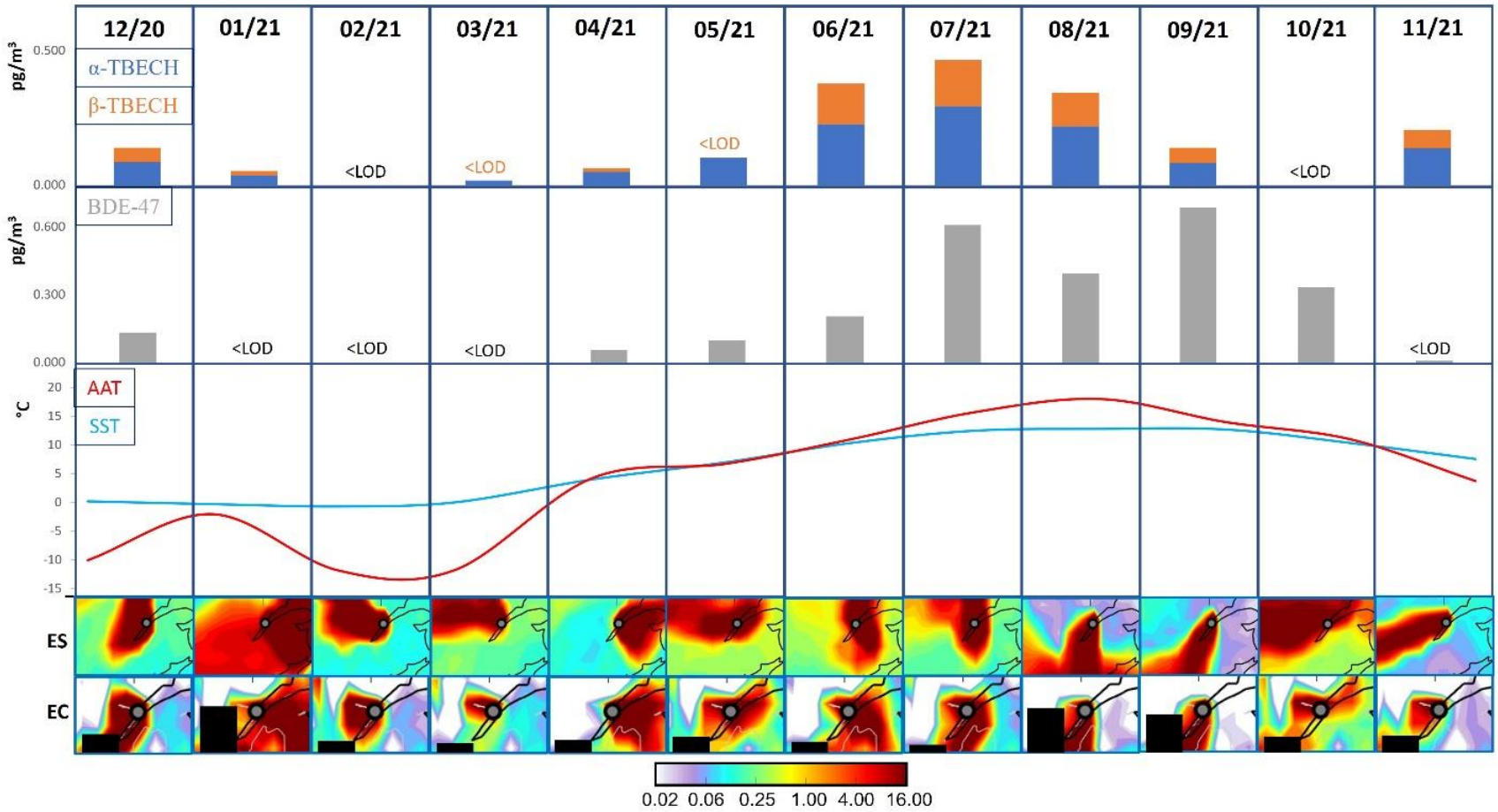

Figure S9 The seasonal variation of the air concentration (gas phase only) of α- and β-TBECH (stacked) and BDE-47 in Tadoussac, QC (top) and the average surface sea (SST) and air temperature (AAT) taken during each sampling period (middle). Similar to Saturna Island, the ES and EC FLEXPART maps of Tadoussac during the sampling period are shown (bottom).

Text S8 Investigating the influence of air mass origin on the concentrations of BFRs measured during active air sampling (AAS) in Saturna Island and Tadoussac

Figures S8 and S9 display the seasonal variability in the concentration of α- and β-TBECH and BDE-47 as measured by AAS on Saturna Island and in Tadoussac, respectively. Also shown are the average air and sea surface temperature at the two sites. In order to shed further light on the source of the variability in these concentrations, we used FLEXPART, a Lagrangian particle dispersion model (Pisso et al., 2019), to determine the history of the air masses sampled on Saturna Island, BC and Tadoussac, QC. FLEXPART was driven by global model-level meteorological data from the European Centre for Medium-Range Weather Forecasts (ECMWF) with 1° × 1° resolution and 3 hourly fields. The model releases 100 000 so-called tracer particles equally throughout the measurement period (24 h for BC and QC; 1 week for ON). The model was then operated backwards in time (20 days) from the starting measurement date to calculate the trajectories of these particles, accounting for the turbulence, convection, and diffusion during the time period. From these simulations, maps identifying the possible source regions were constructed, which were expressed as emission sensitivities (ES) in ns m^{-3}, i.e., the residence time normalized by the volume, in the footprint layer (0-100 m above ground level). The ES maps included in Figs. S8 and S9 therefore illustrates the probability of an airmass to take up pollutants from sources near the ground at a given location.

By multiplying the ES with the annual mean anthropogenic carbon monoxide (CO) emission inventory in the region (obtained from the ECLIPSE database), a modelled CO concentration above the background in the region can be calculated for each sampling period in the three AAS sites. Overlaying the concentrations on a map indicates the potential anthropogenic emission contribution (EC) in the region. Since CO acts like a passive tracer and is correlated with anthropogenic emissions, anthropogenic sources of TBECH and legacy BFRs would also be correlated with the CO emission. Details of the calculations and assumptions used are explained in another study (Sauvage et al., 2017). The EC maps are also included in Figs. S8 and S9.

The FLEXPART ES and EC maps, which indicate the origin of the air mass arriving to Saturna Island and the predicted concentration of CO at the measurement site, i.e., indicate where and how much the sampled air mass could have picked up anthropogenic emissions on its path, can be used to estimate how much anthropogenic emissions impacts the levels of BFRs in this remote region.

In the summer season (June, July, August), the air during the sampling period arrived on Saturna Island directly from the Pacific Ocean, and therefore had little contact with populated areas, which also resulted in very low predicted CO concentrations (Figure S8). This matches with the corresponding TBECH levels that were below the LOD in June and July but does not fit with the fairly high levels measured in August. The air sampled in the colder season (May, October, November, and December) had passed through populated areas (Seattle, Vancouver) and had higher predicted CO concentrations, but the TBECH levels were either in the middle or below the LOD.

Therefore, TBECH may be subjected to complex, competing influences of air mass origin and temperature: Emissions of TBECH are somewhat temperature dependent and are higher in summer and lower in winter. In the studied region, summer air comes from the Pacific Ocean and winter air from the continent. In

other words, there is a seasonal variation in the levels of TBECH and a synchronous variation in the contact of the air mass with populated regions, which interact, and to some extent, cancel each other out. However, the variation of the BDE-47 levels in Saturna Island seems to be less reliant on air mass origin, and more dependent solely on air temperature.

Furthermore, the predicted CO levels from the FLEXPART simulations (Figure S9) at times reflected the relative levels of TBECH in Tadoussac (August to November 2021). However, the air mass origin was not able to explain all variations, e.g., the highest levels of TBECH recorded (July 2021) corresponded to the lowest predicted CO level.

Figure S10 The spatial distribution of the water concentration of α- (top) and β- (bottom) TBECH in British Columbia. A close-up map of Victoria is shown (left) for a detailed view of the clustered sites. For sites with multiple measurements, the average water concentration is used and displayed on the map. Measurements of the air concentrations that were below the LOD (α-TBECH: 11; β-TBECH: 17) are marked in blue. Measurements of air concentrations that were above the LOD but could not be reliably quantified, i.e., below the LOQ (α-TBECH: 3; β-TBECH: 4), are marked in orange. Measurements above the LOQ are marked in yellow.

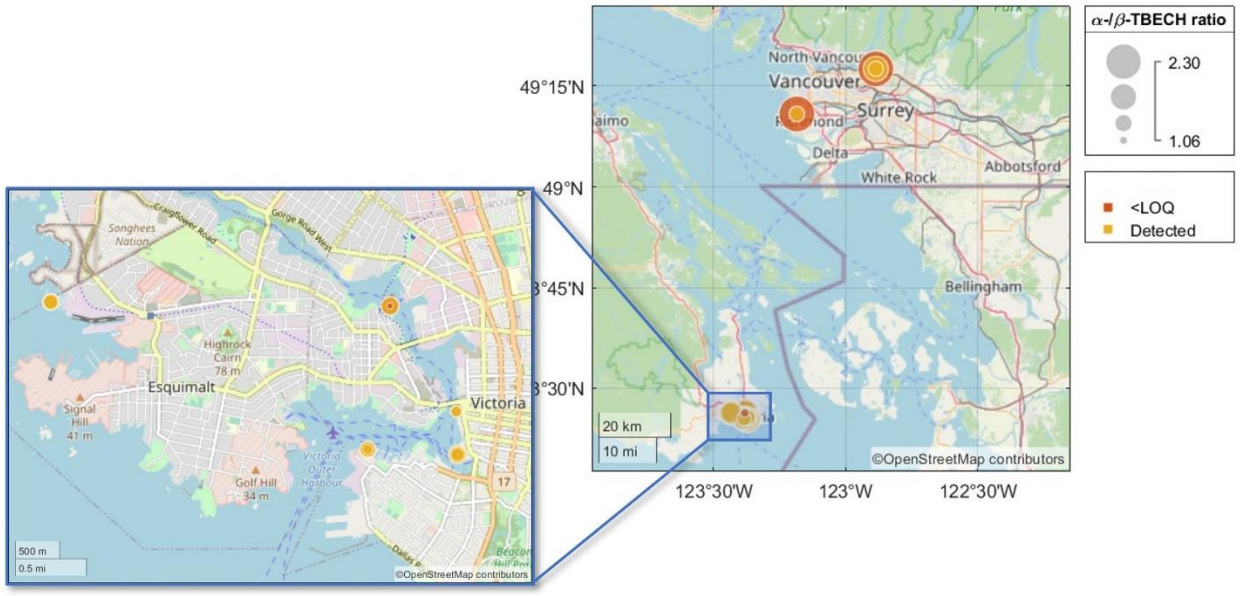

Figure S11 The spatial distribution of the α-/β-TBECH ratios at the PWS sites in British Columbia. A close-up map of the Victoria is shown (left) for a detailed view of the clustered sites. To calculate the ratios, only measurements that were above the LOD for both isomers were used, including measurements that were above the LOD but below the LOQ. To distinguish their certainty, ratios that were calculated using quantifiable measurements and ratios that were calculated using at least one measurement below the LOQ are marked in yellow and orange, respectively.

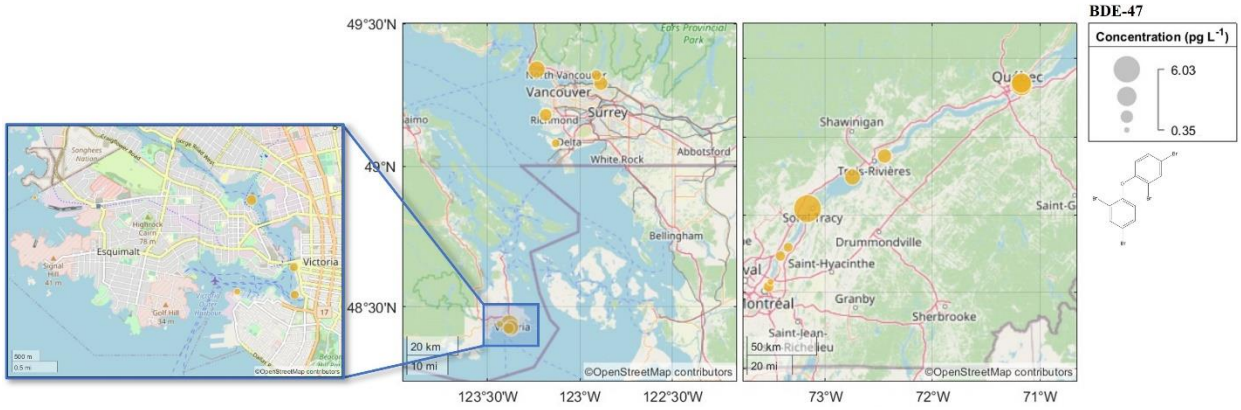

Figure S12 The spatial distribution of the water concentration of BDE-47 in British Columbia (left) and Quebec (right). A close-up map of Victoria is shown (left) for a detailed view of the clustered sites. For sites with replicate measurements, the average water concentration is used and displayed on the map.

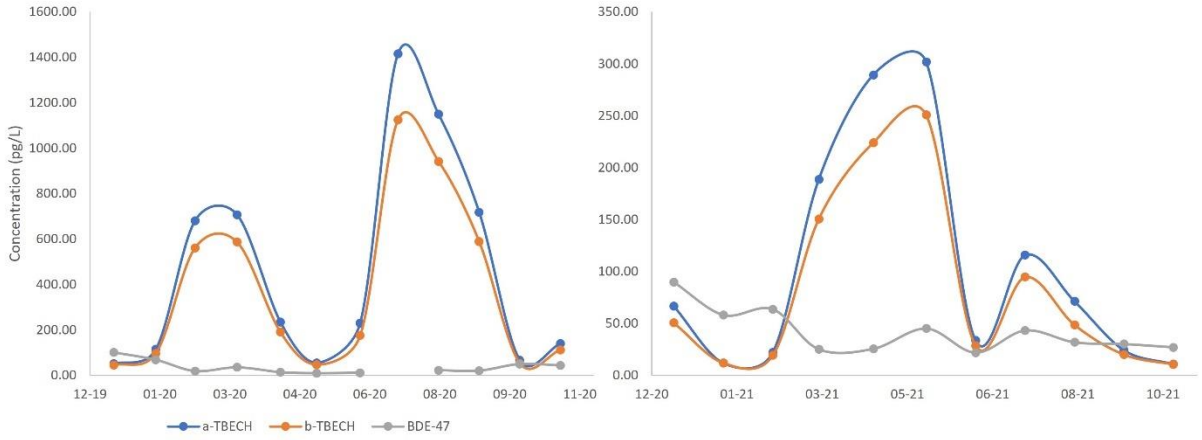

Figure S13 The seasonal variation of α- and β-TBECH and BDE-47 concentration in precipitation samples from Saturna Island, BC (left) and Tadoussac, QC (right).

Table S18 The enantiomeric fraction (EF) of α-TBECH in the air at selected BC and QC sites.

Site name	EF	Site name	EF	Site name	EF	Site name	EF
BC		**BC**		**BC**		**QC**	
L1_2	0.462	L9	0.511	L21	0.469	S25	0.460
L2	0.322	L10	0.525	L22	0.548	S38	0.556
L5_2	0.651	L12	0.507	L23	0.497	S40	0.507
L5_3	0.496	L13_2	0.587	L27	0.575	S51	0.434
L6	0.660	L14	0.611	L28	0.544	S52	0.483
L7	0.425	L18	0.584	L41_2	0.484	S67	0.418
L7_2	0.339	L19	0.604	L45_2	0.478	S68	0.346

Table S19 The enantiomeric fraction (EF) of α-TBECH in the active air samples from Toronto.

Sample	Date	EF	Sample	Date	EF	Sample	Date	EF
AAS1	2020-06-24	0.588	AAS14	2020-09-23	0.579	AAS29	2021-01-06	0.630
AAS2	2020-07-01	0.564	AAS15	2020-09-30	0.521	AAS30	2021-01-13	0.536
AAS3	2020-07-08	0.714	AAS16	2020-10-07	0.521	AAS31	2021-01-20	0.541
AAS4	2020-07-15	0.529	AAS17	2020-10-14	0.552	AAS32	2021-01-27	0.528
AAS5	2020-07-22	0.532	AAS18	2020-10-21	0.669	AAS34	2021-02-10	0.687
AAS6	2020-07-29	0.509	AAS19	2020-10-28	0.556	AAS35	2021-02-17	0.651
AAS7	2020-08-05	0.549	AAS20	2020-11-04	0.629	AAS36	2021-02-24	0.640
AAS8	2020-08-12	0.521	AAS22	2020-11-18	0.676	AAS37	2021-03-03	0.595
AAS9	2020-08-19	0.514	AAS23	2020-11-25	0.604	AAS38	2021-03-10	0.525
AAS10	2020-08-26	0.511	AAS24	2020-12-02	0.628	AAS39	2021-03-17	0.516
AAS11	2020-09-02	0.600	AAS26	2020-12-16	0.440	AAS40	2021-03-24	0.533
AAS13	2020-09-16	0.570	AAS27	2020-12-23	0.665	AAS41	2021-03-31	0.540

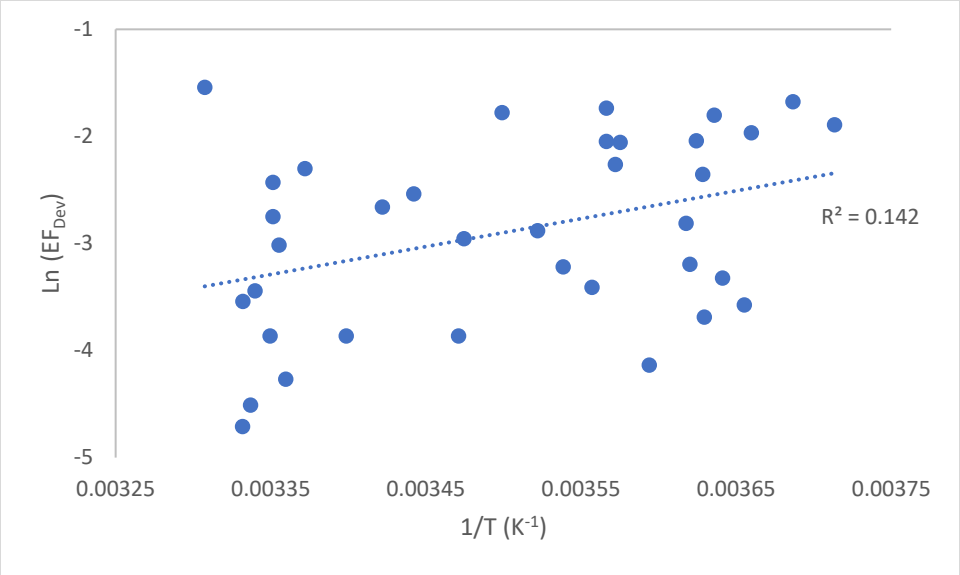

Figure S14 The temperature dependence of the EF deviation from 0.50 (EF_{dev}) in Toronto air.

Table S20 The linear regression parameters for Figure S14.

		Coefficient	Std. error	*t*	*P*	(Adjusted) R^2	Significance F
α-TBECH	Intercept	-12.01	3.85	-3.12	0.0037	(0.12) 0.14	0.023
	x-variable	2603.51	1097.58	2.37	0.023		

Table S21 The enantiomeric fraction (EF) of α-TBECH in the passive water samples.

Site name	EF
V1_Mid	0.451
V9_Mid	0.460
V9_Bot	0.452
V10_Top	0.434
V10_Mid	0.470
V10_Bot	0.426

Text S9 Calculating water-air fugacity ratios and scavenging ratios

Comparing the relative values of the fugacities of a compound between multiple phases is a simple method to determine the net direction of exchange across the interface between phases, as chemicals diffuse from phases with high fugacity to those with low fugacity. With equal fugacities, equilibrium is achieved between the phases; therefore, the ratio of the fugacities in different phases also indicates the extent of deviation from equilibrium.

The fugacity of a compound in phase x (Pa) can be obtained from its volumetric concentration (C_x, mol m^{-3}):

$$f_x = \frac{C_x}{Z_x} \quad (1)$$

where Z_x is the fugacity capacity of the compound in phase x (mol $Pa^{-1}m^{-3}$).

Between two different phases x and y, diffusive exchange of the compound occurs at the interface of the phases, with the higher exchange range occurring from the phase with higher fugacity to that with lower fugacity. The ratio between the fugacities indicates the net direction of exchange. If the exchange between the phases occurs at equal rates, then the fugacities in the two phases are identical, i.e., the fugacity ratio is equal to one. Therefore, the fugacity capacity of a compound in phase x can be determined using the fugacity capacity of a compound in phase y and the partition ratio (K_{xy}) of the two phases:

$$Z_x = K_{xy} Z_y \quad (2)$$

For the fugacity capacity of a compound in air, the value can be derived from the ideal gas law (Z_{air} = 1/RT), which can be used in eq. 2 to find Z_{water} in a water-air system:

$$Z_{water} = \frac{1}{RTK_{aw}} \quad (3)$$

Using eq. 1 and 3, the water-air fugacity ratio can be calculated with eq 4:

$$f_{water}/f_{air} = \frac{C_{water}}{C_{air}} K_{aw} \quad (4)$$

where C_{water} and C_{air} are the volumetric concentration of the compound in water and air, respectively. Therefore, to investigate the diffusive gas exchange of the BFRs across the air-water interface, the water-air fugacity ratio was calculated for the PWS sites with measurements >LOD in BC, by multiplying the K_{AW} with the ratio of the water and air concentrations. Air measurements taken during the PWS campaign period from PAS sites located closest to each PWS site were used in this analysis. K_{AW} values for TBECH and BDE-47 were taken from COSMOtherm predictions (Table 1) and Cetin and Odabasi (2005), respectively.

The scavenging ratio (SR) of a compound is the ratio of the total precipitation concentration (C_{prec}) to the total air concentration (C_{air}) of the compound:

$$SR = \frac{C_{prec}}{C_{air}} \quad (5)$$

The SRs of the BFRs were calculated for each sampling month with precipitation and air measurements >LOD in BC and QC.

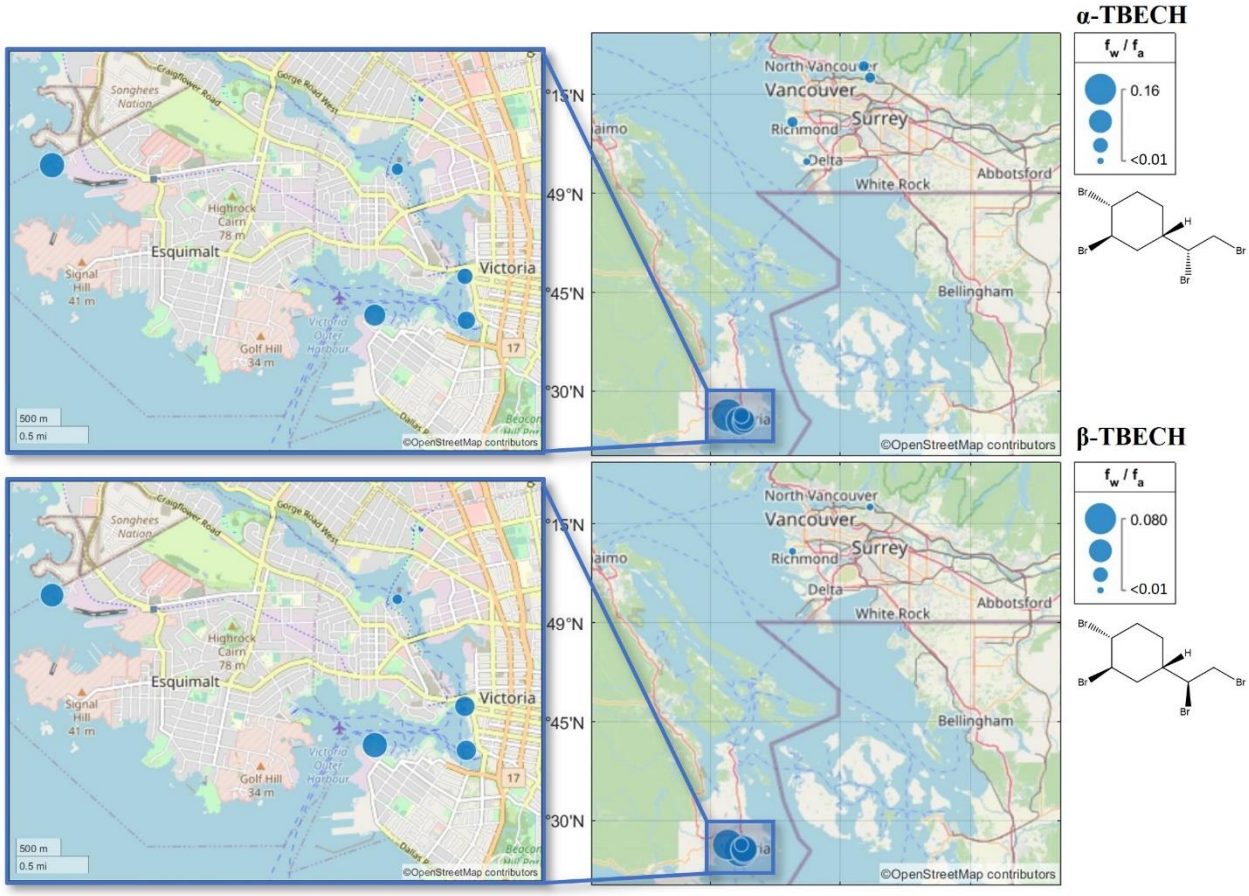

Figure S15 The spatial distribution of the water-air fugacity ratios of α-TBECH (top) and β-TBECH (bottom) at the passive water sampling sites in British Columbia.

Figure S16 The spatial distribution of the water-air fugacity ratios of BDE-47 at the passive water sampling sites in British Columbia and Quebec.

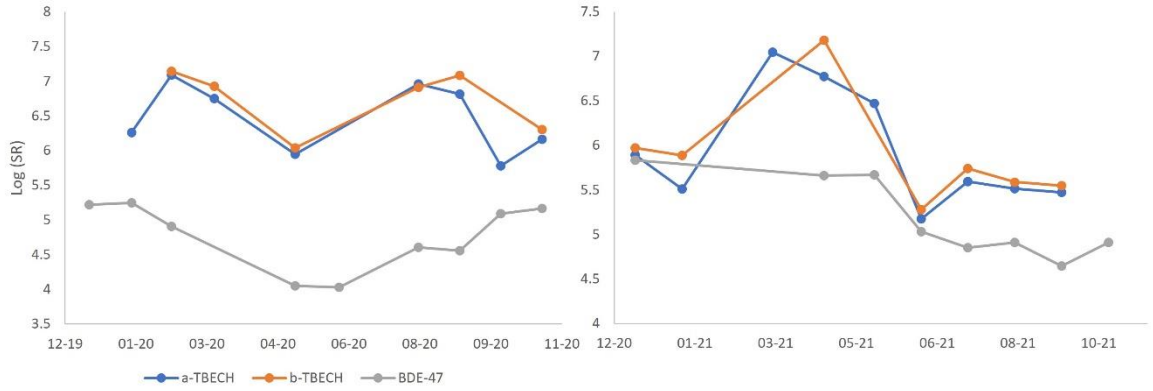

Figure S17 The seasonal variation of the logarithmic scavenging ratios (SRs) of α-and β-TBECH and BDE-47 in Saturna Island (left) and Tadoussac (right).

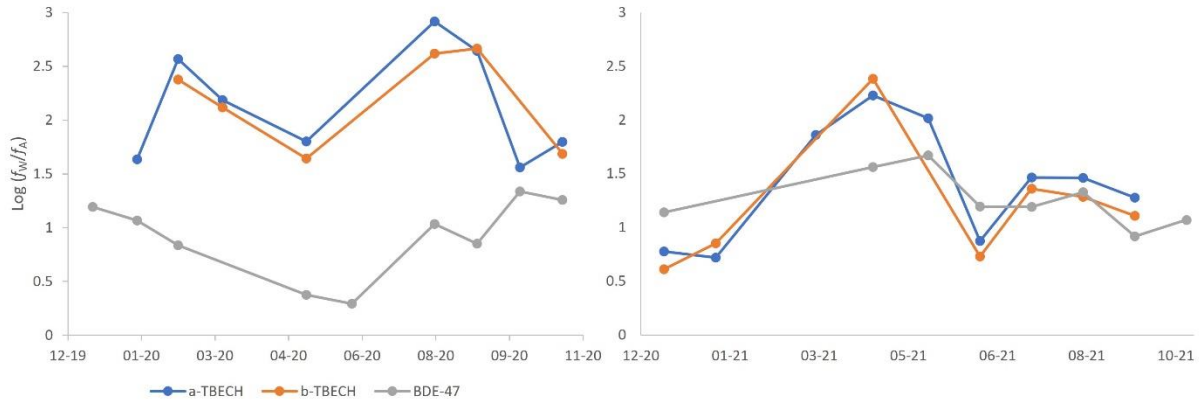

Figure S18 The seasonal variation of the logarithmic water (precipitation)-air fugacity ratios of α-and β-TBECH and BDE-47 in Saturna Island (left) and Tadoussac (right).

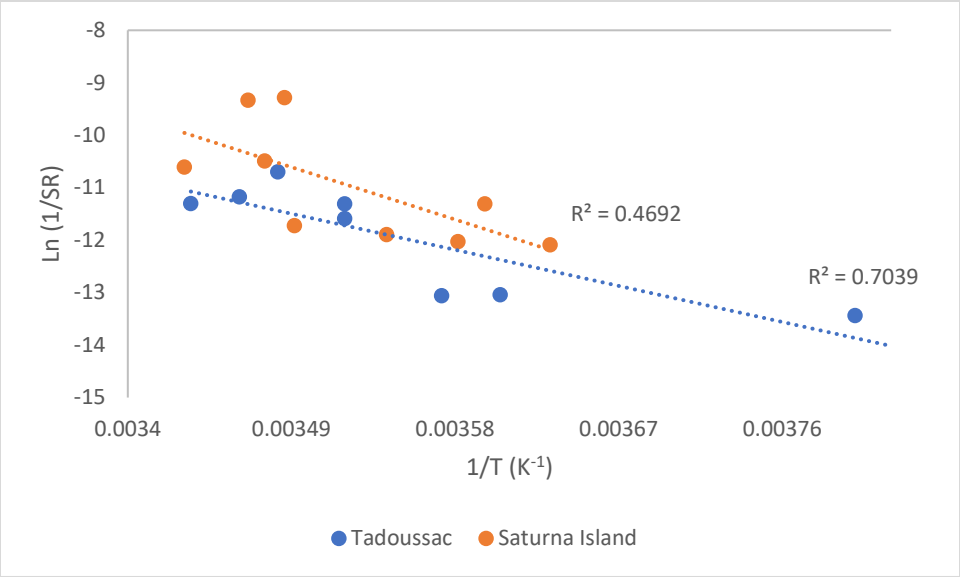

Figure S19 The temperature dependence of the scavenging ratio of BDE-47 in Tadoussac, QC and Saturna Island, BC.

Table S22 Linear regression parameters for the temperature dependence of the scavenging ratio

		Coefficient	Std. error	*t*	*P*	(Adjusted) R^2	Significance F
Saturna Island, BC (x-variable: 1/AAT; y-variable: Ln(1/SR))							
α-TBECH (n=8)	Intercept	-8.47	21.56	-0.39	0.71	(-0.15) 0.015	0.78
	x-variable	-1822.57	6103.68	-0.30	0.78		
β-TBECH (n=6)	Intercept	-2.00	23.93	-0.084	0.94	(-0.16) 0.074	0.60
	x-variable	-3837.91	6796.33	-0.56	0.60		
BDE-47 (n=9)	Intercept	28.08	15.70	1.79	0.12	(0.39) 0.47	0.042
	x-variable	-11084.00	4455.90	-2.49	0.042		
Tadoussac, QC (x-variable: 1/AAT; y-variable: Ln(1/SR))							
α-TBECH (n=9)	Intercept	7.58	11.92	0.64	0.54	(0.21) 0.31	0.12
	x-variable	-5906.97	3309.58	-1.78	0.12		
β-TBECH (n=7)	Intercept	0.18	15.68	0.011	0.99	(-0.040) 0.13	0.42
	x-variable	-3845.99	4389.22	-0.88	0.42		
BDE-47 (n=8)	Intercept	15.18	7.19	2.11	0.079	(0.65) 0.70	0.009
	x-variable	-7642.51	2023.49	-3.78	0.009		

References

Arsenault, G., Lough, A., Marvin, C., McAlees, A., McCrindle, R., MacInnis, G., Pleskach, K., Potter, D., Riddell, N., Sverko, E., Tittlemier, S., and Tomy, G.: Structure characterization and thermal stabilities of the isomers of the brominated flame retardant 1,2-dibromo-4-(1,2-dibromoethyl)cyclohexane, Chemosphere, 72, 1163-1170, https://doi.org/10.1016/j.chemosphere.2008.03.044, 2008.

Bohlin, P., Audy, O., Škrdlíková, L., Kukučka, P., Přibylová, P., Prokeš, R., Vojta, Š., and Klánová, J.: Outdoor passive air monitoring of semi volatile organic compounds (SVOCs): a critical evaluation of performance and limitations of polyurethane foam (PUF) disks, Environ. Sci. Processes Impacts, 16, 433-444, https://doi.org/10.1039/C3EM00644A, 2014.

Booij, K. and Smedes, F.: An Improved Method for Estimating in Situ Sampling Rates of Nonpolar Passive Samplers, Environ. Sci. Technol., 44, 6789-6794, https://doi.org/10.1021/es101321v, 2010.

Canada, S.: Census Profile, 2021: Canada, Provinces and Territories, Statistics Canada, https://www12.statcan.gc.ca/census-recensement/2021/dp-pd/prof/details/download-telecharger.cfm?Lang=E, 2021.

Carlsson, P., Vrana, B., Sobotka, J., Borgå, K., Bohlin Nizzetto, P., and Varpe, Ø.: New brominated flame retardants and dechlorane plus in the Arctic: Local sources and bioaccumulation potential in marine benthos, Chemosphere, 211, 1193-1202, https://doi.org/10.1016/j.chemosphere.2018.07.158, 2018.

Cequier, E., Ionas, A. C., Covaci, A., Marcé, R. M., Becher, G., and Thomsen, C.: Occurrence of a Broad Range of Legacy and Emerging Flame Retardants in Indoor Environments in Norway, Environ. Sci. Technol., 48, 6827-6835, https://doi.org/10.1021/es500516u, 2014.

Cetin, B. and Odabasi, M.: Measurement of Henry's law constants of seven polybrominated diphenyl ether (PBDE) congeners as a function of temperature, Atmos. Environ., 39, 5273-5280, https://doi.org/10.1016/j.atmosenv.2005.05.029, 2005.

Drage, D. S., Newton, S., de Wit, C. A., and Harrad, S.: Concentrations of legacy and emerging flame retardants in air and soil on a transect in the UK West Midlands, Chemosphere, 148, 195-203, https://doi.org/10.1016/j.chemosphere.2016.01.034, 2016.

Genisoglu, M., Sofuoglu, A., Kurt-Karakus, P. B., Birgul, A., and Sofuoglu, S. C.: Brominated flame retardants in a computer technical service: Indoor air gas phase, submicron (PM1) and coarse (PM10) particles, associated inhalation exposure, and settled dust, Chemosphere, 231, 216-224, https://doi.org/10.1016/j.chemosphere.2019.05.077, 2019.

Hong, W.-J., Jia, H., Ding, Y., Li, W.-L., and Li, Y.-F.: Polychlorinated biphenyls (PCBs) and halogenated flame retardants (HFRs) in multi-matrices from an electronic waste (e-waste) recycling site in Northern China, J. Mater. Cycles Waste Manage., 20, 80-90, https://doi.org/10.1007/s10163-016-0550-8, 2018.

Khawar, M. I. and Nabi, D.: Relook on the Linear Free Energy Relationships Describing the Partitioning Behavior of Diverse Chemicals for Polyethylene Water Passive Samplers, ACS Omega, 6, 5221-5232, https://doi.org/10.1021/acsomega.0c05179, 2021.

Klamt, A., Eckert, F., and Diedenhofen, M.: Prediction or partition coefficients and activity coefficients of two branched compounds using COSMOtherm, Fluid Phase Equilibria, 285, 15-18, https://doi.org/10.1016/j.fluid.2009.05.010, 2009.

Li, Y., Zhan, F., Lei, Y. D., Shunthirasingham, C., Hung, H., and Wania, F.: Field Calibration and PAS-SIM Model Evaluation of the XAD-Based Passive Air Sampler for Semi-Volatile Organic Compounds, Environ. Sci. Technol., 57, 9224-9233, https://doi.org/10.1021/acs.est.3c00809, 2023.

Ma, W.-L., Li, W.-L., Zhang, Z.-F., Liu, L.-Y., Song, W.-W., Huo, C.-Y., Yuan, Y.-X., and Li, Y.-F.: Occurrence and source apportionment of atmospheric halogenated flame retardants in Lhasa City in the Tibetan Plateau, China, Sci. Total Environ., 607-608, 1109-1116, https://doi.org/10.1016/j.scitotenv.2017.07.112, 2017.

Melymuk, L., Bohlin-Nizzetto, P., Kukučka, P., Vojta, Š., Kalina, J., Čupr, P., and Klánová, J.: Seasonality and indoor/outdoor relationships of flame retardants and PCBs in residential air, Environ. Pollut., 218, 392-401, https://doi.org/10.1016/j.envpol.2016.07.018, 2016.
NASA: Earth Science Data Systems, NASA [dataset], https://www.earthdata.nasa.gov/, 2015.
Newton, S., Sellström, U., and de Wit, C. A.: Emerging Flame Retardants, PBDEs, and HBCDDs in Indoor and Outdoor Media in Stockholm, Sweden, Environ. Sci. Technol., 49, 2912-2920, https://doi.org/10.1021/es505946e, 2015.
Newton, S., Sellström, U., Harrad, S., Yu, G., and de Wit, C. A.: Comparisons of indoor active and passive air sampling methods for emerging and legacy halogenated flame retardants in Beijing, China offices, Emerging Contam., 2, 80-88, https://doi.org/10.1016/j.emcon.2016.02.001, 2016.
Pisso, I., Sollum, E., Grythe, H., Kristiansen, N. I., Cassiani, M., Eckhardt, S., Arnold, D., Morton, D., Thompson, R. L., Groot Zwaaftink, C. D., Evangeliou, N., Sodemann, H., Haimberger, L., Henne, S., Brunner, D., Burkhart, J. F., Fouilloux, A., Brioude, J., Philipp, A., Seibert, P., and Stohl, A.: The Lagrangian particle dispersion model FLEXPART version 10.4, Geosci. Model Dev., 12, 4955-4997, https://doi.org/10.5194/gmd-12-4955-2019, 2019.
Sauvage, B., Fontaine, A., Eckhardt, S., Auby, A., Boulanger, D., Petetin, H., Paugam, R., Athier, G., Cousin, J. M., Darras, S., Nédélec, P., Stohl, A., Turquety, S., Cammas, J. P., and Thouret, V.: Source attribution using FLEXPART and carbon monoxide emission inventories: SOFT-IO version 1.0, Atmos. Chem. Phys., 17, 15271-15292, https://doi.org/10.5194/acp-17-15271-2017, 2017.
Shoeib, M., Ahrens, L., Jantunen, L., and Harner, T.: Concentrations in air of organobromine, organochlorine and organophosphate flame retardants in Toronto, Canada, Atmos. Environ., 99, 140-147, https://doi.org/10.1016/j.atmosenv.2014.09.040, 2014.
Smedes, F., Geertsma, R. W., Zande, T. v. d., and Booij, K.: Polymer−Water Partition Coefficients of Hydrophobic Compounds for Passive Sampling: Application of Cosolvent Models for Validation, Environ. Sci. Technol., 43, 7047-7054, https://doi.org/10.1021/es9009376, 2009.
Tao, F., Abdallah, M. A.-E., and Harrad, S.: Emerging and Legacy Flame Retardants in UK Indoor Air and Dust: Evidence for Replacement of PBDEs by Emerging Flame Retardants?, Environ. Sci. Technol., 50, 13052-13061, https://doi.org/10.1021/acs.est.6b02816, 2016.
UFZ-LSER database v 3.2. 1: http://www.ufz.de/lserd, last access: May 31, 2023.
Wong, F., Kurt-Karakus, P., and Bidleman, T. F.: Fate of Brominated Flame Retardants and Organochlorine Pesticides in Urban Soil: Volatility and Degradation, Environ. Sci. Technol., 46, 2668-2674, https://doi.org/10.1021/es203287x, 2012.
Wong, F., de Wit, C. A., and Newton, S. R.: Concentrations and variability of organophosphate esters, halogenated flame retardants, and polybrominated diphenyl ethers in indoor and outdoor air in Stockholm, Sweden, Environ. Pollut., 240, 514-522, https://doi.org/10.1016/j.envpol.2018.04.086, 2018.
Zhao, J., Wang, P., Wang, C., Fu, M., Li, Y., Yang, R., Fu, J., Hao, Y., Matsiko, J., Zhang, Q., and Jiang, G.: Novel brominated flame retardants in West Antarctic atmosphere (2011–2018): Temporal trends, sources and chiral signature, Sci. Total Environ., 720, 137557, https://doi.org/10.1016/j.scitotenv.2020.137557, 2020.